

Carbon sequestration in the subsoil and the time required to stabilize carbon for climate change mitigation

Carlos A. Sierra^{1,2}, Bernhard Ahrens¹, Martin Bolinder², Maarten C. Braakhekke¹, Sophie von Fromm^{1,3}, Thomas Kätterer², Zhongkui Luo⁴, Nargish Parvin², and Guocheng Wang⁵

¹Max Planck Institute for Biogeochemistry, Germany

²Department of Ecology, Swedish University of Agricultural Sciences, Sweden

³Department of Environmental Science, ETH Zurich, Switzerland

⁴College of Environmental and Resource Sciences, Zhejiang University, Hangzhou, China

⁵Beijing Normal University, Beijing, China

August 31, 2023

Abstract

Soils store large quantities of carbon in the subsoil (below 0.2 m depth) that is generally old and believed to be stabilized over centuries to millennia, which suggests that subsoil carbon sequestration can be used as a strategy for climate change mitigation. In this article, we review the main biophysical processes that contribute to carbon storage in subsoil and the main mathematical models used to represent these processes. Our guiding objective is to review whether a process understanding of soil carbon movement in the vertical profile can help us to assess carbon sequestration potential at timescales relevant for climate change mitigation. Bioturbation, liquid phase transport, belowground carbon inputs, mineral association, and microbial activity, are the main processes contributing to the formation of soil carbon profiles, and these processes are represented in models using the advection-diffusion-reaction paradigm. Based on simulation examples, and measurements from carbon and radiocarbon profiles across biomes, we found that advective and diffusive transport may only play a secondary role in the formation of soil carbon profiles. The difference between vertical root inputs and decomposition seems to play a primary role in determining the shape of carbon change with depth. Using the transit time of carbon to assess the timescales of carbon storage of new inputs, we show that only small quantities of new carbon inputs travel through the depth profile and can be stabilized for time horizons longer than 50 years, implying that activities that promote carbon sequestration in the subsoil must take into consideration the very small quantities that can be stabilized in the long term.

Keywords: Climate change mitigation, soil carbon sequestration, transit time, advection-diffusion-reaction, microbial decomposition, organic matter stabilization, radiocarbon

22 Contents

23	1 Introduction	3
24	2 Processes contributing to the formation of soil carbon profiles	4
25	2.1 Pedoturbation as diffusive vertical movement	4
26	2.2 Advective transport in liquid phase	4
27	2.3 Depth dependence of organic matter input	5
28	2.4 Depth dependence of decomposition and microbial activity	5
29	2.5 Land management practices that affect soil C profiles	6
30	3 Soil carbon profile models	6
31	3.1 A general model of soil carbon transport and decomposition with depth	7
32	3.1.1 Diffusion	7
33	3.1.2 Advection	8
34	3.1.3 Reaction (decomposition)	9
35	3.1.4 Combining transport and decomposition	9
36	3.2 The constant coefficient model and its steady-state solution	10
37	3.3 Numerical example	13
38	4 Assessing C sequestration and the fate of new C inputs	14
39	4.1 Fate, transit time, and carbon sequestration in the subsoil	14
40	4.2 Numerical example	15
41	5 Empirical evidence from soil profiles	16
42	5.1 The shape of the vertical C profile across regions	17
43	5.2 Transit times of C from vertical profiles	17
44	6 Implications for soil C management	18
45	7 Summary and conclusions	19

1 Introduction

Soil carbon stocks below the topsoil (below 0.2 m depth) are not only one of the largest carbon (C) reservoir of the terrestrial surface, but are also relatively old as demonstrated by radiocarbon measurements (Mathieu et al., 2015; He et al., 2016; Shi et al., 2020; Heckman et al., 2022). These radiocarbon measurements along the vertical profile have shown that the age of carbon increases significantly with depth, indicating that carbon may be stabilized for centuries to millennia in the subsoil. It is therefore reasonable to think that soils could act as a large sink for fossil-fuel derived carbon if subsoil carbon sequestration is promoted, particularly in agricultural and managed lands (Rumpel et al., 2012; Button et al., 2022).

The subsoil has a large influence on ecosystem productivity and the supply of ecosystem services. It has been estimated that between 10 and 80% of the nutrient and water requirement of plants are provided by the subsoil (Hinzmann et al., 2021). Carbon stored in subsoils generally contributes to more than half of the total stocks within a soil profile. However, the amount of organic C stored in soil varies among biomes; relative to the first meter, between 43 and 71% of soil organic carbon (SOC) is found at depths below 20 cm (Jobbágy and Jackson, 2000). In agricultural soils, the amount of soil organic carbon stored in subsoils (up to 1 m depth) is similar to that in the topsoil arable layer (Morari et al., 2019). Due to cost limitations and focus on productivity, studies in agroecosystems often consider only the arable layer ($> 90\%$ observations), where most changes in soil C are assumed to occur because C cycling is more dynamic in topsoil compared to deeper soil layers (Bolinder et al., 2020). However, subsoil C is not insensitive to agricultural management practices. There is evidence from long-term field experiments that management practices affect C stocks at decadal timescales in the upper part of the subsoil or even deeper (e.g. Kirchmann et al., 2013; Kätterer et al., 2014; Menichetti et al., 2015; Börjesson et al., 2018; Dal Ferro et al., 2020; Slessarev et al., 2020).

Furthermore, effects on subsoil carbon are evident when comparing annual versus perennial crops with more well developed root systems or versus other deep rooting species (Carter and Gregorich, 2010; Collins et al., 2010; VandenBygaart et al., 2011; Guan et al., 2016). Major land-use changes such as cropland to grassland, or cropland to forest and vice versa, may also in some cases induce changes in subsoil carbon (Guo and Gifford, 2002; Poeplau and Don, 2013). Button et al. (2022) reviewed several other options than the traditional management practices for increasing subsoil C, such as burial of organic matter or biochar addition to the subsoil. There is a need for including subsoil carbon in model-based estimates of carbon sequestration (Button et al., 2022; Hicks Pries et al., 2023), but the mechanisms governing the effect of changes in subsoil carbon are understudied, which has been identified as a major knowledge gap (Lorenz and Lal, 2005; Chenu et al., 2019) while raising awareness of the potential for subsoils to promote SOC sequestration (Kautz et al., 2013; Chen et al., 2018).

Indeed, the use of deep-rooting plant species has been suggested as a land management strategy to promote carbon input to subsoil and thus sequestering soil carbon and mitigating climate change in cropping systems (Kell, 2011; Thorup-Kristensen et al., 2020). However, there are mixed results regarding the time new carbon inputs to subsoil would be stabilized on decadal timescales. Recent quantifications of the transit time of carbon inputs across soil depth showed that carbon inputs transit fast in all soil layer depths, challenging the efficiency of promoting carbon inputs to subsoil for soil carbon sequestration (Xiao et al., 2022; Wang et al., 2023a).

Managing soils for C sequestration purposes implies that the fate and transit time of new carbon inputs can be accurately quantified (Crow and Sierra, 2022). Mathematical models of subsoil carbon dynamics play an important role for this purpose, and can be used to estimate the amount and persistence of new carbon due to land management.

In this review, we survey the main processes that contribute to soil carbon storage and dynamics in the subsoil, with particular emphasis on mathematical models of subsoil carbon dynamics. Our guiding question is whether a process understanding of soil C movement through the vertical profile can help us to assess C storage and persistence at timescales relevant for climate change mitigation. For this purpose, we first review process understanding of subsoil C dynamics, and then review mathematical models used in the past to represent these processes. Based on this review, we show that most previous models can be generalized under one single modeling paradigm, and through examples, show the main

contribution of different processes in shaping soil carbon profiles. In addition, we present a conceptual framework to assess the fate of new carbon inputs as they move through the subsoil. We use the theoretical framework provided by the transit time distribution of carbon in compartmental systems (Sierra et al., 2017, 2018b; Metzler and Sierra, 2018), and discuss our results in the context of soil carbon management for climate change mitigation.

2 Processes contributing to the formation of soil carbon profiles

A number of physical, chemical, and biological processes contribute to the formation of soil carbon profiles, which have been reviewed with some detail elsewhere (e.g. Button et al., 2022; Hicks Pries et al., 2023). Here, we briefly review some of these processes grouping them according to their most common representation in models. Our objective is to make a parallel between process understanding and mathematical representations in models, which are reviewed in section 3.

2.1 Pedoturbation as diffusive vertical movement

Processes that mix the soil are commonly referred to as pedoturbation (Hole, 1961; Fey and Schaetzl, 2017), which include the reworking activity of soil fauna (bioturbation), freezing and thawing cycles (cryoturbation) (Johnson et al., 1987; Bockheim, 2007; Beer et al., 2022), uprooting of trees (Schaetzl et al., 1990), swelling and translocation of clays (Finke, 2012), and human disturbances such as tillage (Fey and Schaetzl, 2017; Keyvanshokouhi et al., 2019). Bioturbation and tillage are the pedoturbation processes most commonly considered in models of soil carbon profiles, mostly represented in analogy to particle diffusion.

Soil mixing by bioturbation has a homogenizing effect on soil properties: it increases dispersal of particles, reduces concentration gradients, and destroys layering (Johnson et al., 1987). Hence, bioturbation leads to organic matter diffusion and potentially to deepening of the soil profile. In croplands, tillage contributes to vertical mixing of soil carbon, altering the depth distribution of root inputs and aboveground residues (Luo et al., 2010). Depending on ploughing depth, the effects of tillage may only concentrate on the topsoil and may be difficult to observe at depths below 40 cm (Luo et al., 2010; Keyvanshokouhi et al., 2019; Mary et al., 2020).

2.2 Advective transport in liquid phase

A small part of organic matter in soils is dissolved in the liquid phase. Concentrations of dissolved organic carbon (DOC) are typically so low that total organic carbon in solution is negligible compared to the immobile fraction (Michalzik et al., 2001). However, leaching and decomposition fluxes of dissolved organic matter may be important terms in shaping the dynamics of soil carbon at depth (Neff and Asner, 2001; Kalbitz and Kaiser, 2008; Kindler et al., 2011; Kaiser and Kalbitz, 2012). DOC is highly relevant for the formation of the soil profile since it is subject to potentially very fast transport with downward water fluxes and represents a mechanism of organic matter input at depths well below the zone where bioturbation and root input are relevant (Rumpel et al., 2012). Furthermore, adsorption of DOC to the mineral phase is one of the main mechanisms for organic carbon stabilization and persistence (Kalbitz and Kaiser, 2008).

The concentration of DOC in soils covaries with precipitation (Liu et al., 2021) as water acts as the main medium for DOC transport. Therefore, rates of vertical water movement are commonly used to estimate DOC vertical transfer as an advective process (Ota et al., 2013).

A considerable part of DOC is easily degradable, with low molecular weight compounds decreasing strongly with depth (Roth et al., 2019). An important mechanism for DOC removal is immobilization due to interactions with the solid phase and (co-)precipitation. Through a range of chemical mechanisms, DOC is adsorbed to surfaces of minerals (particularly Al and Fe hydroxides and clay) and to a lesser extent to solid organic matter (Neff and Asner, 2001; Kalbitz and Kaiser, 2008).

2.3 Depth dependence of organic matter input

The relative distribution of litter input between above- and belowground fractions, as well as the vertical distribution of the belowground input, is highly relevant for the carbon profile. Jobbágy and Jackson (2000) found a significant relationship between vertical soil carbon distribution and plant functional type, which is partially explained by ecosystem-level root/shoot ratios and the vertical distribution of root biomass. Since net primary production (NPP) is the source of litter input, its distribution over above- and below-ground biomass is a good predictor of the relative proportions of aboveground litter fall and rhizodeposition (Raich and Nadelhoffer, 1989; Xiao et al., 2023).

Synthesizing global data sets including NPP measurements from 725 soil profiles, root biomass and its depth distribution from 559 soil profiles, Xiao et al. (2023) recently mapped depth-resolved belowground NPP (BNPP) at 1 km resolution across the globe. They found that global average BNPP allocated to the 0–20 cm soil layer is estimated to be $1.1 \text{ Mg C ha}^{-1} \text{ yr}^{-1}$, accounting for $\sim 60\%$ of total BNPP. Across the globe, the depth distribution of BNPP varies largely but mostly follows a decreasing trend with depth, and more BNPP is allocated to deeper layers in hotter and drier regions. The highest levels of BNPP and carbon inputs to subsoil are in tropical and subtropical latitudes as well as in temperate forests and grasslands, while lowest levels of BNPP are in deserts and high latitude regions (Xiao et al., 2023).

In croplands, the belowground distribution of root inputs is associated with crop type and whether annual or perennial cropping systems are in place (Mosier et al., 2021; Hicks Pries et al., 2023). In a review for temperate agricultural crops, Fan et al. (2016) showed that 50% of the roots mostly accumulate in the upper 8 – 20 cm, and Bolinder et al. (2007) found that about 20% of total NPP is allocated aboveground and 50% belowground in common annual agricultural crops.

Independent of vegetation or crop type, root distribution seems to be mostly determined by soil hydrology, as demonstrated by significant relationships between annual potential evapotranspiration, precipitation, and soil texture (Schenk and Jackson, 2002a). In more water limited ecosystems, plants tend to have deeper root profiles to maximize water uptake (Schenk and Jackson, 2002b). Roots may also preferentially grow in the organic surface layer, if present, due to the high nutrient and moisture availability there (Jordan and Escalante, 1980; Schenk and Jackson, 2002a).

2.4 Depth dependence of decomposition and microbial activity

A distinct property of most soils is the decrease of radiocarbon (^{14}C) activity with depth, indicating a higher average age of carbon since plant uptake from the atmosphere and a decrease in decomposition rates with depth (Mathieu et al., 2015; He et al., 2016; Lawrence et al., 2020; Rumpel and Kögel-Knabner, 2011; Heckman et al., 2022; Scheibe et al., 2023; Hicks Pries et al., 2023). Potential factors responsible for this age gradient include the slow downward transport of carbon fractions that are either very recalcitrant, or recurrently recycled by microbes (Elzein and Balesdent, 1995; Gleixner, 2013; Kaiser and Kalbitz, 2012; Roth et al., 2019); decreasing microbial activity along the profile (Jenkinson and Coleman, 2008; Persson et al., 2000; Koven et al., 2013; Wang et al., 2021), and increasing role of organo-mineral associations with depth (Rumpel and Kögel-Knabner, 2011; Eusterhues et al., 2003; Rasmussen et al., 2018; Cotrufo and Lavalley, 2022; Georgiou et al., 2022; Hicks Pries et al., 2023). The reason for this gradient is not fully understood yet and needs further exploration (Guo et al., 2023). It may be caused by the selective preservation of recalcitrant compounds combined with downward transport (Elzein and Balesdent, 1995; Luo et al., 2020) as well as nonlinear interactions among C fractions such as priming (Guenet et al., 2013; Liang et al., 2018; Wang et al., 2021).

A further cause of stabilization in deep soil is physical disconnection between microbes and substrates (Don et al., 2013; Gleixner, 2013). Most microbial activity in deep soils is located in so-called hot spots: root and earthworm channels and preferential water flow paths (e.g. cracks). Organic matter outside of these zones may be stabilized due to spatial separation from decomposers (Chabbi et al., 2009).

2.5 Land management practices that affect soil C profiles

The distribution of C along the vertical profile can be modified by management practices on agriculture, rangeland, and forest soils. Historically, the management and cultivation of soils have resulted in a significant carbon loss of about 133 PgC (Sanderman et al., 2017). Hicks Pries et al. (2023) categorize management practices that affect subsoil carbon in three groups, physical redistribution due to tillage, changes in the vertical distribution of root inputs due to vegetation change, and addition of exogenous C inputs applied at the surface or buried at depth. These practices tend to modify the physical mixing of particles in soil, the transport of water and advective movement of C, and the vertical distribution of root inputs and microbial activity.

Practices that alter the physical structure of soils such as tillage constantly redistribute organic matter between top and subsoil, acting as a mechanism for the diffusion of organic and mineral-associated carbon particles (Keyvanshokouhi et al., 2019; Mary et al., 2020; Button et al., 2022). Deep ploughing (Alcántara et al., 2016; Wang et al., 2023b) or deep soil flipping (Schiedung et al., 2019) have also an important impact on the vertical distribution of C, but their sporadic application is more challenging to represent in models, particularly using equations for advection.

Vegetation change due to management alters the partitioning of primary production between above and belowground components, and also the vertical distribution of root inputs and rhizodeposition (Rumpel and Kögel-Knabner, 2011). In models, changes in vegetation can have an influence on the total amount of carbon inputs entering the soil system, the shape of the decline of root inputs by depth, its partitioning between labile and stable fractions, and the production of DOC (Ota et al., 2013).

Exogenous C inputs such as biochar, compost or biosolids to subsoil can be considered as C inputs differing in chemical and physical properties in comparison to regular C inputs from roots (Paustian et al., 2016). They alter the total amount and the vertical distribution of inputs to soils, and can modify rates of microbial activity if the new inputs are highly degraded or strongly bound to mineral surfaces (Rumpel et al., 2012; Button et al., 2022).

3 Soil carbon profile models

While the overwhelming majority of soil carbon models do not represent spatial processes (Manzoni and Porporato, 2009), a small number of models have been published that in some way account for the vertical soil carbon profile. For example, some models vertically distribute simulated total soil organic carbon or extrapolate topsoil carbon downwards using a predefined depth-function, in order to determine lateral soil carbon transport due to erosion (Rosenbloom et al., 2001; Hilinski, 2001). Several models represent carbon pools in predefined soil layers that differ with respect to physical and chemical parameters, as well as temperature, moisture, and root input (van Veen and Paul, 1981; Grant et al., 1993). In some cases heat or water transport between layers is included to account for the effects of temperature and moisture on decomposition, or to simulate leaching of mineral nitrogen (Hansen et al., 1991; Li et al., 1992). However, these models do not consider explicitly vertical transfer of organic matter between layers. A number of models of DOC dynamics have been proposed (Michalzik et al., 2003; Neff and Asner, 2001; Gjettermann et al., 2008; Brovelli et al., 2012). These models account explicitly for production and mineralization of DOC, as well as vertical transport with water flow and ad- and desorption. Transport is usually represented as advection, based on measured or simulated water fluxes. These schemes are mainly developed to reproduce DOC fluxes and concentrations at small scales, and usually require site level calibration or detailed information on soil texture.

The effects of bioturbation in terrestrial soils have been modeled in relation to transport of radionuclides (e.g. Müller-Lemans and van Dorp, 1996; Kaste et al., 2007; Bunzl, 2002) and soil formation (Kirkby, 1977; Salvador-Blanes et al., 2007). More literature exists on modelling of benthic bioturbation and its effects on chemical species in sediments at the bottom of oceans and lakes (e.g. Boudreau, 1986a; Meysman et al., 2005, 2010; Sarmiento and Gruber, 2006; Arndt et al., 2013). Bioturbation in these systems is usually modeled as a diffusive process, although it has been shown that this approach is not generally valid (Meysman et al., 2003, 2010). Alternatively, other schemes have been

proposed to represent diffusive processes, which includes both deterministic (Boudreau, 1986b, 1989) and stochastic approaches (Bunzl, 2002; Choi et al., 2002; Meysman et al., 2008).

Perhaps the first model truly aimed at dynamically simulating the soil carbon profile was developed by Kirkby (1977), as part of a soil formation model. Since then, a number of models have been developed that combine decomposition with vertical transport, represented either as diffusion (O'Brien and Stout, 1978; van Dam et al., 1997; Koven et al., 2009), advection (Nakane and Shinozaki, 1978; Dörr and Münnich, 1989; Bosatta and Ågren, 1996; Feng et al., 1999; Baisden et al., 2002; Jenkinson and Coleman, 2008), or both (Elzein and Balesdent, 1995; Bruun et al., 2007; Freier et al., 2010; Guenet et al., 2013; Koven et al., 2013; Braakhekke et al., 2011, 2013). Most of these models were developed to explain measurements of carbon and tracer profiles. Increasingly, more models are now developed to represent soil carbon cycling and predict land-atmosphere carbon exchange (Huang et al., 2018; Koven et al., 2013; Tifafi et al., 2018; Ahrens et al., 2020; Luo et al., 2020; Wang et al., 2021), and the effect of land management practices on carbon sequestration in soils (Jenkinson and Coleman, 2008; Taghizadeh-Toosi et al., 2014; Keyvanshokouhi et al., 2019; Mary et al., 2020).

3.1 A general model of soil carbon transport and decomposition with depth

The main processes involved in the formation of soil carbon profiles, bioturbation, liquid phase transport, rhizodeposition, and decomposition, are commonly represented in models using the mathematical paradigms of diffusion, advection, and reaction, respectively. It is therefore useful to conceptualize models of SOM transport and dynamics by a general paradigm expressed as

$$\frac{\partial x(d, t)}{\partial t} = \text{Diffusion} + \text{Advection} + \text{Reaction}, \quad (1)$$

where the variable x represents soil organic matter or carbon, and variable t represents time. We use here partial derivatives (the ∂ symbol) to represent the change of soil carbon with respect to time, assuming that it can also change along a variable d that denotes soil depth. Therefore, we are also interested in representing changes in x with depth; i.e. $\partial x / \partial d$. Equation 1 is a continuity equation, expressing how the conserved quantity x , which obeys mass conservation, changes continually with soil depth and time.

Our main postulate is that all models of vertical SOC transport are special cases of 1, expressing different forms of diffusion, advection and reaction. This general approach to modeling vertical dynamics has been identified previously for diverse systems such as marine organic matter (Sarmiento and Gruber, 2006) or sediments (Arndt et al., 2013).

3.1.1 Diffusion

Processes related to bioturbation and tillage are commonly represented in models using diffusion equations. A simple general model of soil carbon profile dynamics including only vertical diffusion and inputs can be expressed as

$$\frac{\partial x(d, t)}{\partial t} = \frac{\partial}{\partial d} \left(\kappa(d, t) \frac{\partial x(d, t)}{\partial d} \right) + u(d, t), \quad (2)$$

where $\kappa(d, t)$ is a function that represents how mass diffusivity depends on soil depth and time. Mass diffusivity is a soil property that generally does not change considerably over short timescales. Some models represent changes in diffusion with depth as a function of bulk density. In the most simple case it can be expressed as a constant κ with no depth dependence. The function $u(d, t)$ expresses how litter and root inputs change with depth and time, and can take multiple forms depending on attributes of the vegetation such as phenology, allocation, and rhizodeposition.

Models of the form of equation 2 can only be solved (analytically or numerically) if initial conditions $x(d, 0)$ are known as well as the carbon contents or their change at two points along the vertical profile, between a depth at the surface d_0 and some maximum depth d_{\max} . The latter are called the boundary conditions, and must be known a priori in order to obtain solutions of these models.

To obtain an intuitive understanding of potential solutions to this model, it is useful to assume mass diffusivity as a constant (κ) and that inputs of organic matter to the soil are constant over time according to some function $u(d)$ where the inputs change with depth. Under these conditions, the soil carbon content along the profile reaches a steady-state in which it does not change over time; i.e.,

$$\frac{\partial x(d, t)}{\partial t} = 0,$$

and the steady-state carbon content along the profile $x(d)$ is the solution to the second order ordinary-differential equation

$$\frac{\partial^2 x}{\partial d^2} = -\frac{u(d)}{\kappa}. \quad (3)$$

Again, this equation can be solved using boundary conditions, integrating with respect to d to obtain the distribution of carbon content with depth $x(d)$. Equation 3 implies that the steady-state carbon content in a diffusion controlled environment is mostly defined by the relation between the depth distribution of inputs and the mass diffusivity of the soil. The vertical distribution of inputs is mostly a property of the vegetation and the rhizosphere system, while mass diffusivity is mostly a property of the soil and the organisms that act as bio-engineers.

3.1.2 Advection

The other main mathematical paradigm used to represent vertical processes in soil carbon profiles is advection; i.e., the transport of organic carbon dissolved in water. Following mass conservation, advection can be expressed as

$$\frac{\partial x(d, t)}{\partial t} = -\frac{\partial}{\partial d} f(x(d, t)), \quad (4)$$

where $f(x(d, t))$ is the flux or flow rate of mass at depth d and time t . In other words, the mass of soil carbon can only change over time due to the flow rate of the fluid along a vertical direction. If the fluid is flowing at a constant velocity v , equation 4 can be simplified to

$$\frac{\partial x(d, t)}{\partial t} = -v \frac{\partial x(d, t)}{\partial d}. \quad (5)$$

Intuitively, this implies that soil carbon is removed from a depth d at the velocity at which the fluid is passing through, and the gradient at which carbon content changes with depth. Flow velocity is determined by the combination of all the physical, chemical, and biological factors that affect water flow in saturated and unsaturated soils. Although flow velocity may not be constant in most cases, equation 5 helps to understand its role in modeling SOM transport mechanisms in soils.

To better understand the role of $f(x(d, t))$ in equation 4, it is useful to think of $x(d, t)$ as a density function (LeVeque, 1990) that represents the mass concentration of SOM at a particular depth and time. Therefore, the total mass of carbon between two depths d_1 and d_2 at time t is given by

$$\int_{d_1}^{d_2} x(d, t) dd.$$

Because in an advection only system the total mass between the depths d_1 and d_2 only changes due to the flux at the end points, we can assume that

$$\frac{d}{dt} \int_{d_1}^{d_2} x(d, t) dd = f(x(d_1, t)) - f(x(d_2, t)). \quad (6)$$

The function $x(d, t)$ is not known explicitly, therefore we do not have explicit formulas for the flow rates f . Nevertheless, equation 6 helps to understand the role of the flow rate function f in equation 4; it represents the flow rate of soil carbon at any given depth and time.

3.1.3 Reaction (decomposition)

If we ignore vertical transport, soil carbon would display temporal dynamics related to the action of microorganisms and how they consume organic matter. This process of decomposition has been studied extensively, and there are hundreds of mathematical models that represent these dynamics ignoring vertical transport processes (Manzoni and Porporato, 2009). Despite the large variety of models, most of these models can be expressed in a general expression of the form (Sierra and Müller, 2015; Sierra et al., 2018a)

$$\frac{d\mathbf{x}}{dt} = \mathbf{u}(\mathbf{x}, t) + \mathbf{B}(\mathbf{x}, t) \cdot \mathbf{x}(t). \quad (7)$$

This general model is expressed in vector (lower case bold) and matrix (upper case bold) form because it is assumed that soil organic carbon is highly heterogeneous, and different proportions decompose at different rates. Therefore, the vector $\mathbf{x}(t) \in \mathbb{R}^n$ represents the mass of soil carbon in n number of compartments at time t . The total mass at time t , $x(t)$, can be simply obtained as the sum of the elements of this vector, i.e. $x(t) = \|\mathbf{x}(t)\|$ (the vertical bars represent a norm and indicate a sum of the positive elements of a vector). Mass inputs to this system are represented by the vector $\mathbf{u}(\mathbf{x}, t)$, which expresses the amount of organic matter inputs that would enter each compartment. Because above and belowground litter inputs can differ in their chemical and physical properties, different proportions of the total mass may enter different compartments. In addition, the inputs may depend on the amount of carbon in particular compartments; for example, if exudation rates depend on the amount of mycorrhiza. For this reason, the inputs \mathbf{u} are expressed as dependent on the amount of mass present in the compartments at any given time.

Rates of decomposition and transfer of carbon among compartments are expressed in the matrix $\mathbf{B}(\mathbf{x}, t)$ of equation 7. This matrix is called compartmental because it has important mathematical properties related to mass conservation: all diagonal elements are non-positive, all off-diagonal elements are non-negative, and the column sums are non-positive (Metzler and Sierra, 2018; Sierra et al., 2018a).

Linear models such as Century and RothC as well as nonlinear microbial models such as those proposed by soil ecologists (e.g Schimel and Weintraub, 2003; Allison et al., 2010) are especial cases of the general model of equation 7 (Sierra and Müller, 2015), whose internal structure helps to study particular aspects of decomposition processes that are independent of vertical transport. These processes include: differences in the decomposability of different types of organic matter, organo-mineral interactions, effects of abiotic variables such as temperature, moisture, and pH on the rates of organic matter processing, interactions between substrates and microbial groups, among others.

To incorporate vertical transport processes in this model, we can assume that at any given depth d , reaction (decomposition) processes are expressed as

$$\frac{\partial x(d, t)}{\partial t} = \left\| \frac{d\mathbf{x}(d, t)}{dt} \right\| \quad (8)$$

where the sum is over all the compartment contents at any given depth and time. Notice that this expression contains all the litter inputs entering the soil, split according to the compartments at which they enter.

3.1.4 Combining transport and decomposition

In the previous sections, we analyzed the processes of diffusion, advection, and decomposition separately. Now we can combine them following the general paradigm expressed in equation 1. This general model has the form

$$\begin{aligned} \frac{\partial x(d, t)}{\partial t} &= \frac{\partial}{\partial d} \left(\kappa(d, t) \frac{\partial x(d, t)}{\partial d} \right) - \frac{\partial}{\partial d} f(x(d, t)) + \left\| \frac{d\mathbf{x}(d, t)}{dt} \right\|, \\ &= \frac{\partial}{\partial d} \left(\kappa(d, t) \frac{\partial x(d, t)}{\partial d} \right) - \frac{\partial}{\partial d} f(x(d, t)) + \|(\mathbf{u}(\mathbf{x}, d, t) + \mathbf{B}(\mathbf{x}, d, t) \cdot \mathbf{x}(d, t))\|. \end{aligned} \quad (9)$$

Most mathematical models of vertical carbon transport and decomposition should be special cases of this equation. It can lead to very complex dynamics resulting from the simultaneous effect of physical, chemical and biological processes related to transport and decomposition.

Equation 9 cannot be solved analytically, but it can be discretized in time and space to obtain numerical solutions. The discretization approach consists of defining a fixed number k of depth intervals Δd where the solution of the partial differential equation is approximated using algebraic equations, and the system is then moved forward in time at discrete intervals Δt . Most numerical methods to approximate solutions to equation 9 would attempt to find a vector $\mathbf{X} \in \mathbb{R}^{k+2}$ for k depth intervals by solving a linear equation of the form

$$\mathbf{A} \cdot \mathbf{X} = \mathbf{F}, \quad (10)$$

where the matrix \mathbf{A} and the vector \mathbf{F} result from the discretization of the original system using a finite-difference or a finite-element method (Lanczos, 1996; LeVeque, 2007). The dimension of this system is $(k+2) \times (k+2)$, with the 2 additional dimensions incorporating information based on the boundary conditions, which must be added to the discretized system and become an integral part of the new linear differential operator (Lanczos, 1996). Because after the discretization mass conservation must be preserved, we postulate that the new system of equations must be compartmental. In other words, a discretized system representing transport and decomposition of organic matter can be expressed as a compartmental system of the form of equation 7. There are a few examples from the previous literature that may help to confirm this assertion. For instance, Metzler et al. (2020) showed that the soil carbon module of the ELM model (Koven et al., 2013), which contains 10 discrete depth layers and 7 pools in each layer, can be approximated with a compartmental system that produces the exact same numerical solution as the original model that was developed with partial differential equations. Similarly, (Huang et al., 2018) expressed the same model of Koven et al. (2013) as a system of linear equations in matrix form and found exact approximations to the original model.

The approximation of the nonlinear model expressed with partial differential equations is possible if the system is assumed at steady-state. In the general model of equation 9, the steady state solution $x_{ss}(d)$ is obtained when $\partial x(d, t)/\partial t = 0$. At this steady-state, the amount of carbon stored in the system does not change over time and nonlinear interactions vanish. Therefore, the behavior of $x_{ss}(d)$ and a tracer such as ^{14}C , which is commonly used to parameterize SOC transport models, becomes linear with constant coefficients (Anderson, 2013). Thus, models of SOC dynamics with vertical transport can be expressed as linear systems with compartmental structure assuming the system is at near steady-state.

3.2 The constant coefficient model and its steady-state solution

Despite the generality of the model of equation (9) to represent vertical patterns of diffusion and advection, most of the models previously reported in the literature use constant diffusion and advection as well as constant decomposition and transformation rates (Table 1). Furthermore, most previous studies solve the model for the steady-state carbon content and analyze the resulting vertical patterns. Therefore, it is important to study in more detail a simplified version of the general model of equation 9 for the case of constant coefficients at the steady-state.

Assuming constant diffusion ($\kappa(d, t) = \kappa$ for all d and t), and constant flow velocity ($f(x(d, t) = vx(d)$, with v constant for all d and t), we can write a steady-state version of equation 9 by making the time derivative equal to zero as

$$\kappa \frac{\partial^2 x(d)}{\partial d^2} - v \frac{\partial x(d)}{\partial d} + g(d) = 0, \quad (11)$$

with $g(d)$ representing the balance between inputs and decomposition at each depth, also assuming constant decomposition and transformation rates at each depth ($\mathbf{B}(\mathbf{x}, d, t) = \mathbf{B}(d)$ for all \mathbf{x} , and t), and a constant vector of inputs at each depth ($\mathbf{u}(\mathbf{x}, d, t) = \mathbf{u}(d)$ for all \mathbf{x} and t). Therefore,

$$g(d) = \|\mathbf{u}(d) + \mathbf{B}(d) \cdot \mathbf{x}(d)\|. \quad (12)$$

Equation 11 is a general form of a linear second order differential equation with constant coefficients, for which a numerical solution can be obtained by discretizing the system along fixed depth intervals and solving the resulting system of linear equations as in equation 10.

Two further simplified forms of the general equation can be found in the literature. The case in which advective transport is not considered relevant (e.g. O'Brien and Stout, 1978) and therefore

$$\kappa \frac{\partial^2 x(d)}{\partial d^2} + g(d) = 0, \quad (13)$$

or the case in which diffusive transport is not considered relevant (e.g. Feng et al., 1999; Baisden et al., 2002; Baisden and Parfitt, 2007)

$$-v \frac{\partial x(d)}{\partial d} + g(d) = 0. \quad (14)$$

To interpret data from pulse response experiments, some researchers have ignored the inputs and decomposition part of the model (e.g. Bruun et al., 2007) using an equation of the form

$$\kappa \frac{\partial^2 x(d)}{\partial d^2} - v \frac{\partial x(d)}{\partial d} = 0. \quad (15)$$

Models explicitly representing decomposition usually use one or three pools to represent decomposition as in most traditional first order pool models. More detailed representations of decomposition are presented in the model of Braakhekke et al. (2011, 2013), which represents five different pools, including a litter layer component clearly separating processes related to decomposition in the surface organic layer from processes more affected by vertical transport in the mineral horizons. Also, the model of Koven et al. (2013) used 7 distinct C pools: coarse woody debris, three litter pools, and three mineral soil C pools.

In the COMISSION model, not only advective DOC transport is considered, but also advective transport of litter particles similarly as in sediment models (Ahrens et al., 2015, 2020). In the latest version of the model (Ahrens et al., 2020), advective litter transfer and particle diffusion are depth dependent. The model also consider non-linear interactions among C pools, therefore it deviates from the constant linear coefficients model of equation 11 and is in better analogy to equation 9. Similarly, the model of Wang et al. (2021) includes nonlinear interactions among C pools, with the size of the microbial biomass pools interacting with the size of litter and mineral soil pools, but ignoring advection and treating diffusion as a constant across all depths.

Table 1: Summary of models representing C dynamics along the vertical profile using the advection-diffusion-reaction paradigm. Modified and updated from Koven et al. (2013).

Model/reference	Mathematical form	d_{\max} (m)	Ecosystem/location	n	v	κ	Péclet number
O'Brien and Stout (1978)	Eq. 13	1.00	Managed pasture, NZ	1		$13.2 \text{ cm}^2 \text{ yr}^{-1}$	0
Elzein and Balesdent (1995)	Eq. 11	1.65	Kattinkar, India	3	0.13 mm yr^{-1}	$5.15 \text{ cm}^2 \text{ yr}^{-1}$	0.003
Elzein and Balesdent (1995)	Eq. 11	1.95	Pará, Brazil	3	0.34 mm yr^{-1}	$16.58 \text{ cm}^2 \text{ yr}^{-1}$	0.002
Elzein and Balesdent (1995)	Eq. 11	1.63	Bahia, Brazil	3	0.48 mm yr^{-1}	$5.29 \text{ cm}^2 \text{ yr}^{-1}$	0.009
Elzein and Balesdent (1995)	Eq. 11	0.52	Forest, Bezange, France	3	0.6 mm yr^{-1}	$0.94 \text{ cm}^2 \text{ yr}^{-1}$	0.064
Elzein and Balesdent (1995)	Eq. 11	1.00	Forest, Marly, France	3	0.42 mm yr^{-1}	$1.48 \text{ cm}^2 \text{ yr}^{-1}$	0.028
Feng et al. (1999)	Eq. 14	1.00	Oak chaparral, USA	1	1.51 cm yr^{-1}		∞
Feng et al. (1999)	Eq. 14	1.00	Pine, USA	1	1.67 cm yr^{-1}		∞
Feng et al. (1999)	Eq. 14	1.00	Ceanothus chaparral, USA	1	1.56 cm yr^{-1}		∞
Feng et al. (1999)	Eq. 14	1.00	Chamise chaparral, USA	1	1.52 cm yr^{-1}		∞
Baisden et al. (2002) ¹	Eq. 14		< 3 ky old grassland soil, USA	3	$[4.0, 0.47, 0.40] \text{ mm yr}^{-1}$		∞
Baisden et al. (2002)	Eq. 14		200 ky old grassland soil, USA	3	$[4.0, 0.49, 0.39] \text{ mm yr}^{-1}$		∞
Baisden et al. (2002)	Eq. 14		600 ky old grassland soil, USA	3	$[3.2, 0.28, 0.43] \text{ mm yr}^{-1}$		∞
Baisden et al. (2002)	Eq. 14		3 My old grassland soil, USA	3	$[0.5, 0.26, 0.10] \text{ mm yr}^{-1}$		∞
Bruun et al. (2007)	Eq. 15	0.55	Cropland, Denmark	0	$0.0081 \text{ cm yr}^{-1}$	$0.71 \text{ cm}^2 \text{ yr}^{-1}$	0.011
Baisden and Parfitt (2007)	Eq. 14	1.00	15 ky old grassland soil, NZ	3	$[6.2, 0.9, 0.19] \text{ mm yr}^{-1}$		∞
Baisden and Parfitt (2007)	Eq. 14	1.00	200 ky old grassland soil, NZ	3	$[0.6, 1.3, 0.25] \text{ mm yr}^{-1}$		∞
Baisden and Parfitt (2007)	Eq. 14	1.00	600 ky old grassland soil, NZ	3	$[0.5, 0.5, 0.5] \text{ mm yr}^{-1}$		∞
Braakhekke et al. (2011)	Eq. 11	0.7	Deciduous forest, Germany	5	0.002 m yr^{-1}	$0.6 \text{ cm}^2 \text{ yr}^{-1}$ ²	0.333
Ota et al. (2013)	Eq. 11	1.5	Mediterranean grassland, USA	3			NA
Braakhekke et al. (2013)	Eq. 11	2.0	Pine forest, Netherlands	5	0.0651 m yr^{-1}	$0.0852 \text{ cm}^2 \text{ yr}^{-1}$	76.402
Braakhekke et al. (2013)	Eq. 11	0.7	Deciduous forest, Germany	5	$0.00137 \text{ m yr}^{-1}$	$0.6792 \text{ cm}^2 \text{ yr}^{-1}$	0.202
Koven et al. (2013)	Eq. 13	3.8	Global, non-permafrost	7		$1 \text{ cm}^2 \text{ yr}^{-1}$	0
Ahrens et al. (2015)	Eq. 11	0.9	Coniferous forest, Germany	4	NA	$3.24 \times 10^{-10} \text{ m}^2 \text{ s}^{-1}$	NA
Wang et al. (2021)	Eq. 13	1.2	Global, non-permafrost	7		$8.55 \times 10^{-5} \text{ cm}^2 \text{ h}^{-1}$	0

¹The model considers three separate values of v for each C pool

²Assuming a bulk density of 1000 kg cm^{-3}

Particularly interesting is the model of Elzein and Balesdent (1995), which follows the form of equation 11 and includes advection, diffusion, and decomposition of three distinct pools. This model is rather useful because it includes a minimum of complexity to represent most relevant processes of a carbon transport model. It is also a useful model for parameterization against data on C and ^{14}C concentrations in vertical profiles.

Returning to our steady-state analysis of the constant coefficient model, we can solve the system for the first derivative and analyze individual components of this equation

$$\frac{\partial x(d)}{\partial d} = \frac{\kappa}{v} \frac{\partial^2 x(d)}{\partial d^2} + \frac{g(d)}{v}. \quad (16)$$

For the special case of one single pool with vertical root inputs represented by $u(d)$ and vertical decomposition rates by $k(d)$,

$$\frac{\partial x(d)}{\partial d} = \frac{\kappa}{v} \frac{\partial^2 x(d)}{\partial d^2} + \frac{u(d) - k(d)x(d)}{v}. \quad (17)$$

Equation 17 is very useful to analyze the shape of soil C profiles for cases in which the equilibrium assumption is reasonable. First, equation 17 shows that the vertical change of C in a soil profile is inversely proportional to the advective movement of C such as in the case of DOC transport. For large values of advection velocity (v) the rate of change of C by depth would be small and the vertical C profile would resemble a vertical line. Second, the sign of the rate of change of C by depth is mostly determined by the difference between belowground C inputs and decomposition. At depths where the decomposition flux ($k(d) x(d)$) is larger than belowground inputs, the decrease of C by depth is maximum (maximum negative value). Third, the ratio between diffusion and advection velocity (κ/v), the inverse of the Péclet number (see below), influences how second order transport processes affect the shape of the rate of change of the vertical C profile (Figure 1).

In the analysis of partial differential equations, the Péclet number, defined as the ratio of advection to diffusion, plays a very important role in determining characteristics of the solution such as its numerical stability (LeVeque, 2007). In addition, the Péclet number can be used to determine the degree by which diffusion or advection may dominate the shape of a soil C profile (Figure 1).

If soil C always decreases with depth (Jobbágy and Jackson, 2000), the decomposition flux in equation 17 must be dominant across the entire soil profile so the rate of change with depth remains negative. In fact, this analysis suggests that the balance between lateral C inputs and decomposition is one of the main factors that affect the shape of soil C profiles where a continuous decrease in soil C is commonly observed.

A corollary or implication provided by equation 17 is that if the decrease in soil C with depth follows a simple exponential function, the right hand side of equation 17 must be a constant value for all depths. This situation seems unlikely given the different interacting process that occur in a soil, and in fact, mathematical functions different than the simple exponential provide the best fit to observed data (Jobbágy and Jackson, 2000).

3.3 Numerical example

We used equation 17 to investigate the role of diffusion, advection, decomposition and lateral inputs on the shape of idealized soil carbon profiles. We chose values of κ and v within the range of values obtained in previous models (Table 1) as well as representative functions for $k(d)$ and $u(d)$ within the range of previous studies (e.g. Elzein and Balesdent, 1995; Jackson et al., 1996, 1997; Koven et al., 2013).

To investigate the effect of diffusion and advection, we ran simulations with values of $\kappa = \{0.1, 1, 5, 15\} \text{ cm}^2 \text{ yr}^{-1}$ and $v = \{0.1, 1, 5, 10\} \text{ cm yr}^{-1}$ (Figure 2). The results show that vertical transport processes tend to create a horizon with largest rate of change in concentrations of C with depth (1st derivative) close to the surface. This layer could be the result of either advection or diffusion (Figure 2). Because in these simulations, lateral root inputs and decomposition decrease with depth (see equations 18, and 19 below), there is a general trend of C concentrations to decline to values close to zero. Therefore, vertical transport do not seem to play a major role in transporting carbon below 50 cm depth within

the range of advection and diffusion values used in these simulations, which covers the entire range of values obtained in previous studies (Table 1). Only at high advection velocities ($v = 10 \text{ cm yr}^{-1}$) some carbon is transported below 50 cm depth, but this advection velocity is much higher than what has been used before in other models (Table 1).

The first derivative of the C concentration profiles with respect to depth from these simulations (Figure 2 right panels), showed negative derivatives for the entire depth profile. According to equation 17, the first derivative can only be positive if lateral root inputs and transport processes dominate over the decomposition flux, which is not the case in these simulations. The decomposition flux dominates over all other processes making the first derivative negative although approaching zero at deeper layers. As advection velocity increased, the first derivatives were less negative, indicating that as advective transport increases the change in C concentrations by depth is less pronounced.

In a second set of simulations, we practically removed advection and diffusion by making the value of these coefficients very small ($\kappa = v = 0.01$) and represented lateral root inputs with the function

$$u(d) = -\beta^d \ln \beta. \quad (18)$$

This function predicts vertical root distributions and was originally proposed by Gale and Grigal (1987) and used by Jackson et al. (1996, 1997) to obtain vertical root distributions at the biome level. The original function predicts the fraction of root biomass for each depth, and multiplied by an average root turnover rate of 1 yr^{-1} (Gill and Jackson, 2000), gives the proportion of root inputs per depth interval $u(d)$. For the simulations, we used values of $\beta : \{0.92, 0.95, 0.98\}$ that include the observed extremes of values for shallow root systems ($\beta = 0.92$) and deep root systems ($\beta = 0.98$) (Gale and Grigal, 1987; Jackson et al., 1996).

The function used to represent decomposition rates by depth was extracted from Koven et al. (2013)

$$k(d) = k_0 \exp\left(\frac{-d}{d_e}\right), \quad (19)$$

with the maximum decomposition rate at the surface given by $k_0 = k(d = 0)$, and d_e representing the e-folding depth of decomposition rates. In our simulations, we used values of $k_0 : \{1, 0.1, 0.01\} \text{ yr}^{-1}$ and a constant value of $d_e = 90 \text{ cm}$ (the model showed little sensitivity to different values of d_e).

The results from this second set of simulations evaluating the effect of lateral root inputs and decomposition showed that slowing down decomposition can have a significant effect on the shape of the vertical soil C profile. These results seems counterintuitive because equation 17 suggest that the negative term of the equation should be affected by larger values of $k(d)$, but because with slow decomposition higher amounts of C are obtained at steady-state, the entire term $k(d)x(d)$ is large, promoting a strong soil C gradient. The vertical distribution of root inputs has also a significant effect on the shape of the soil C profile, with shallow root inputs promoting a strong vertical gradient and deep rooting systems a more pronounced gradient with lower values of the first derivative. In this set of simulations, we observed also a maximum rate of change of C at the upper layers where the value of the first derivative reached a maximum.

4 Assessing C sequestration and the fate of new C inputs

4.1 Fate, transit time, and carbon sequestration in the subsoil

In the context of climate change mitigation, we are generally interested in evaluating the capacity of soils for storing carbon at relevant timescales associated with management and policy outcomes. In many cases we are interesting in comparing different soils; and in other cases, we are interested in evaluating the effectiveness of different soil management practices. In any case, we need to use appropriate metrics to evaluate the environmental benefit of carbon sequestration.

If we aim at promoting soil C sequestration, it is then important to analyze the fate of new inputs entering the soil, assess for how long the new carbon remains stored, and how much warming can be avoided while the C is stored (Sierra et al., 2021a; Crow and Sierra, 2022). For this purpose, we

can use the following metrics: fate, transit time, and carbon sequestration, which are mathematically defined as follows.

For a compartmental system in equilibrium, where carbon inputs are balanced with C losses, the fate of C entering at a time t_0 can be obtained as a function that predicts the mass of C remaining in the soil at any given time $t > t_0$ (Sierra et al., 2021b)

$$\mathbf{m}(t) = e^{\tau \mathbf{B}} \mathbf{u}, \quad (20)$$

where $\mathbf{m}(t)$ is a vector with the mass remaining for each compartment. This mass remaining is related to the transit time of carbon, which is defined as the time it takes carbon atoms to pass through the entire network of compartments until C leaves the soil system (Bolin and Rodhe, 1973; Manzoni et al., 2009; Sierra et al., 2018a). The transit time distribution of carbon can be expressed as (Metzler and Sierra, 2018)

$$f_T(\tau) = -\mathbf{1}^\top \mathbf{B} e^{\tau \mathbf{B}} \frac{\mathbf{u}}{\|\mathbf{u}\|}, \quad (21)$$

and represents the relative proportion of carbon leaving the system at a time τ . In soils, transit time distributions generally have a long tail, indicating that most carbon entering soils are respired quickly but small proportions can stay for long times (Sierra et al., 2018b).

Carbon Sequestration (CS) is the storage of a certain amount of carbon over a certain period of time. It evaluates the fate of new inputs entering the soil integrated over a time horizon. The amount of sequestration quantified by the CS metric depends on both the amount of inputs entering the soil and the time it takes this carbon to return to the atmosphere in the form of respiration. This amount of time is proportional to the transit time of carbon.

For a compartmental system at equilibrium, CS can be obtained as (Sierra et al., 2021a)

$$\text{CS}(t) = \int_{t_0}^t \|e^{\tau \mathbf{B}} \mathbf{u}\| d\tau, \quad (22)$$

which is the integral of the total amount of mass remaining in the soil from a cohort of inputs entering at t_0 .

If a particular transport-decomposition model can be discretized and expressed as a compartmental system following standard numerical methods (LeVeque, 2007; Lanczos, 1996), one can use equation 22 to quantify the fate, transit time and CS of a particular soil and compare results with those from another soil, or with the outcomes of different forms of management.

Alternatively, $\mathbf{m}(t)$ and $f_T(\tau)$ can be obtained using impulse response experiments with existing transport models that are difficult to express as a compartmental system (Thompson and Randerson, 1999; Metzler and Sierra, 2018). The approach consists of running a model until reaching equilibrium, and at this point add a pulse of carbon and observe the mass remaining of the pulse over time, which is an approximation to $\mathbf{m}(t)$. One can also observe the respiration flux after the addition of the pulse, which is an approximation to the transit time distribution $f_T(\tau)$ (Metzler and Sierra, 2018). The results from pulse-response experiments should provide very valuable information to assess the fate of new inputs entering the soil and whether they remain for relevant periods of time.

4.2 Numerical example

In the previous example, we saw that transport, decomposition, and lateral root inputs play an important role in determining the shape of soil C profiles at equilibrium. We evaluate now with an example how fast/slow transport, combined with fast/slow decomposition in soil profiles can affect the fate, transit time and carbon sequestration of a soil. Our aim is to assess the fate of new carbon inputs and whether they remain in soil for timescales relevant for climate change mitigation.

Given that our previous example showed that diffusion plays a minor role in comparison to advection for moving carbon downwards, we set a fixed value of $\kappa = 1 \text{ cm}^2 \text{ yr}^{-1}$ and varied the values of v . For simulations with fast transport, the values were $v = 5 \text{ cm yr}^{-1}$, and for simulations with slow transport $v = 0.1 \text{ cm yr}^{-1}$. Decomposition rates were considered fast with values of $k_0 = 1 \text{ yr}^{-1}$ and slow with $k_0 = 0.1 \text{ yr}^{-1}$ at the surface (Table 2) and declining with depth according to equation 19.

Table 2: Parameters used and results obtained for simulations evaluating the effect of transport and decomposition on the fate, transit time and carbon sequestration of new inputs. Tf-Df: transport fast, decomposition fast; Tf-Ds: transport fast, decomposition slow; Ts-Df: transport slow, decomposition fast; Ts-Ds: transport slow, decomposition slow.

	Tf-Df	Tf-Ds	Ts-Df	Ts-Ds
κ (cm ² yr ⁻¹)	1.000	1.000	1.000	1.000
v (cm yr ⁻¹)	5.000	5.000	0.100	0.100
k_0 (yr ⁻¹)	1.000	0.100	1.000	0.100
β	0.950	0.950	0.950	0.950
Proportion remaining after 1 yr	0.449	0.914	0.424	0.875
Proportion remaining after 10 yr	0.002	0.480	0.001	0.392
Proportion remaining after 50 yr	0.000	0.000	0.000	0.022
Mean transit time (yr ⁻¹)	1.333	9.699	1.217	11.498
Median transit time (yr ⁻¹)	0.859	9.444	0.799	7.096
CS($t \rightarrow \infty$)	16.028	363.721	12.587	133.416

In all simulations, we considered a root input profile with an intermediate value of $\beta = 0.95$, i.e. not too shallow nor too deep roots.

Simulation results showed that most C inputs entering at any given time only stay in the soil a few years, and only under slow decomposition, some C may remain for a few decades (Figure 4, Table 2). Decomposition rates seem to play a stronger control on the fate of C inputs than vertical transport rates. Under fast decomposition, most carbon was lost in 5 years independently from transport velocity, and very small proportions travelled through the soil profile because the carbon was decomposed before it had a chance to move downwards. Under slow decomposition and fast transport, some carbon is preserved longer because it decomposes at slower rates at deeper layers, but eventually this transported carbon is also decomposed in a few decades (Figure 4).

The transit time distribution of C through the entire soil profile for these different simulations showed that the large majority of C entering the soil at any given time is lost within the first year (Figure 5a). Fifty percent of the C that enters the soil is lost in 0.86 years in the scenario with fast decomposition and fast transport, while in the scenario with slow decomposition and fast transport 50% of the new carbon is lost in 9.4 years (Table 2). The slow decomposition scenarios showed a very different tail in the transit time distribution compared to the fast decomposition scenarios, with a larger proportion of carbon staying for longer times under slow decomposition. Therefore, the mean transit time is influenced by these long tails, with the mean transit time in the fast transport slow decomposition scenario of 1.3 years, and 11.5 years in the slow transport slow decomposition scenario (Table 2a). Despite slow decomposition however, most of the new inputs do not stay for timescales beyond a few decades at the maximum.

At steady-state, significantly more carbon is stored in the case of slow decomposition, particularly in the scenario of fast transport and slow decomposition (Figure 5b). However, to reach this large steady-state C concentrations, very long timescales of carbon accumulation are required. According to the transit time distributions, very small amounts of new C inputs remain in the long-term, therefore it would take a considerably long time (beyond decades) to reach these steady-state C values.

5 Empirical evidence from soil profiles

The two numerical examples from the previous section suggest that (i) the change of soil C with depth is largely influenced by the difference between root inputs and decomposition, and to a lesser degree by vertical transport processes such as diffusion and advection; (ii) most new carbon inputs entering the soil do not remain stored for long timescales. In the following section, we will explore global-scale datasets of soil C profiles to test whether these theoretical model predictions have empirical support on observations.

5.1 The shape of the vertical C profile across regions

The International Soil Radiocarbon Database (ISRaD) is a comprehensive and well curated collection of soil carbon and radiocarbon data (Lawrence et al., 2020). We used version 1.7.8 of the database and extracted information on soil C concentration with depth down to 1 m. Data from 600 individual profiles were grouped by Köppen-Geiger climate zones (Beck et al., 2018) and averaged by 1 cm depth increments. Volcanic soils (classified as such in the field) were treated as a separate group given their distinct vertical C profile. A mass-preserving spline function (equal-area quadratic smoothing spline) was applied to each profile to account for the varying depth intervals in which samples across profiles were taken (Ponce-Hernandez et al., 1986; Bishop et al., 1999). This spline function interpolates C concentration for a continuum of depths, i.e. an approximation to the function $x(d)$ for each of the groups (Figure 6).

Soil carbon decreased rapidly with depth in most soil profiles reaching values close to zero at 1 m depth (Figure 6), with the exception of soils from tundra/polar regions and volcanic soils, which still contain relatively large quantities of C at 90 cm depth. Please note that these values are reported as concentrations with respect to mass of soil. Bulk density data is not commonly reported for individual profiles and much less for individual depth horizons. Therefore, comparisons with the simulation experiments from previous sections must be done only with respect to qualitative aspects and not with respect to quantitative values.

The first derivative of soil C concentrations with respect to depth ($\partial x(d)/\partial d$, Figure 7) was negative for all groups, indicating that soil C always decreases with depth for these aggregated profiles. This is in agreement with our previous simulations in which the first derivatives were always negative. We observed for all groups a peak in the first derivative where it reaches a maximum negative value, indicating that soil C decreases more strongly at some intermediate depth between 10 and 20 cm (Figure 7). According to equation 17, a maximum negative value of the first derivative can only occur at depths where the microbial decomposition flux ($k(d)x(d)$) has its maximum value, i.e. when microbes are consuming the maximum amount of carbon possible.

The value of the first derivative had the largest values overall for volcanic soils, and the lowest values for arid soils. In both cases decomposition rates may be slow compared to other soils; in volcanic soils the presence of amorphous non-crystalline surfaces promote sorption of organic matter to minerals and therefore slow decomposition and strong C accumulation (Marin-Spiotta et al., 2011; Crow et al., 2015); in arid soils low moisture availability leads to slow decomposition rates, but also low primary productivity leads to low carbon stocks (Moyano et al., 2013; Sierra et al., 2015). Therefore, negative values of the first derivative are strongly dependent on the C stocks ($x(d)$), and to a lesser extend on the decomposition rate ($k(d)$). The decomposition rate obviously plays a major role in determine the size of the C stock in conjunction with the input fluxes at depth, but the rate of decline of C with depth is mostly influenced by the resulting C stock. In addition, the last term of equation 17 also reveals that for systems with slow advection velocities v approaching zero, small differences between lateral inputs and decomposition may be amplified. In other words, the large values of the negative derivative for the volcanic soils may be the result of very low advective movement of DOC, amplifying small differences between lateral inputs and decomposition.

Overall, the data from soil C profiles aggregated by regional groups and volcanic soils provide evidence supporting the idea that vertical transport may play a secondary role in determining the rate of soil C decrease with depth. The difference between lateral root inputs and decomposition may play a primary role in determining the shape of soil C profiles, and this difference may be amplified at low advection velocity rates. Diffusive movement of soil C seems to play a small role in these aggregated groups, something suggested by the low values of the second derivative (Figure 7); however, diffusion may have some control on the peak of C decrease found close to the surface in these profiles.

5.2 Transit times of C from vertical profiles

Using data from ISRaD and a dataset on root input profiles, Xiao et al. (2022) obtained estimates of mean ages and mean transit times for soil C profiles at the global scale. The global averages revealed that mean transit times of C are always younger than the mean age of C stored at all soil depths

(Figure 8). In other words, despite the C stored in the soil being hundreds to thousands of years old, the C respired is only a few years to decades old. This result is consistent with our transit time simulations that showed mean transit times of only a few years (Figure 5, Table 2). However, the actual values of mean transit time obtained from the data are actually much higher than those from the model results. This is to be expected given that the model used for the example only considered one single pool, but in reality soil carbon is highly heterogeneous and a significant proportion of its total carbon cycles at much slower rates, which would contribute to higher transit times. In addition, sorption of OM to mineral surfaces may increase with depth, making the overall decomposition of C at depth more limited (Ahrens et al., 2020). Nevertheless, model simulations and observations agree in that new C inputs to soil only remain stored in timescales of years to decades.

Fast mean transit times were observed for tropical forest, grassland and cropland soils, while long transit times in the order of decades to centuries were only observed for tundra and boreal forest soils (Figure 8). These results are consistent with the idea that low temperatures and energy limitation may play a significant role in controlling the transit time of C at the biome level (Lu et al., 2018; Xiao et al., 2022), with fast transit times in warm regions and longer transit times in cold high-latitude regions.

Because transit times are directly related to Carbon Sequestration CS (equations 21 and 22), we expect only tundra and boreal forest soils to store C in the subsoil at timescales relevant for climate change mitigation, i.e. in the order of decades to centuries. In fact, previous studies have found that a large proportion of carbon used by microorganisms in the subsoil is recent and does not contribute to C stabilization in the subsoil (Balesdent et al., 2018; Scheibe et al., 2023). Therefore, we would expect lower values of CS for tropical forests, grasslands and cropland soils in comparison with boreal forests and tundra soils. However, it is important to keep in mind that productivity in these high-latitude regions is relatively low compared to temperate and equatorial latitudes (Xiao et al., 2023). CS as defined in equation 22 accounts for this trade-off between the amount of inputs and its transit time through the soil, and it can be used to more specifically assess the climate mitigation potential of specific amounts of C added to the soil.

6 Implications for soil C management

Our analysis of a general model of soil C profile formation, together with the analysis of observations of soil carbon concentrations and transit times, provide relevant insights that can inform land management for carbon sequestration and climate change mitigation. Even though current observations show that C concentrations decrease strongly with depth in most soils and new C inputs transit relatively fast, there are potentials to increase C storage with depth and increase the transit time of carbon across the entire profile.

If soils would be managed to increase subsoil C storage, the change of C concentrations with depth should be less dramatic and change less with respect to topsoil. From equation 16, it can be inferred that a management objective could be framed in terms of keeping the first derivative of C concentration with respect to depth close to zero (Figure x). This implies

$$\frac{\partial x(d)}{\partial d} = \frac{\kappa}{v} \frac{\partial^2 x(d)}{\partial^2 d} + \frac{g(d)}{v} = 0, \quad (23)$$

and because the derivative of a constant zero is equals to zero, the second derivative term vanishes from this equation and the management objective reduces to

$$\frac{g(d)}{v} = 0. \quad (24)$$

This equation suggest that an effective way to achieve the goal of increasing C storage with depth is through increasing advective transport of C from top to subsoil; i.e. large values of v approximate the ratio of equation 24 to zero. Provided C inputs are high, their vertical advective movement should contribute to increase total carbon storage. In other words, even though vertical C transfer does not seem to play a significant role in explaining current data on soil C profiles, management activities

could be implemented to increase vertical C transfers to horizons where it can be stabilized in available mineral surfaces (Georgiou et al., 2022) and protected from decomposition. Equation 16 also suggest that a small difference between C inputs and decomposition across all depths ($g(d) \approx 0$) helps to decrease the gradient of C decline with depth. For example, exogenous amendments of organic matter with low decomposition rates could help to reduce this difference and reduce C decline with depth. There may be many other ways to achieve this management goal, and a challenge for future research would be to test this theoretical prediction through different experiments.

7 Summary and conclusions

We reviewed the main processes that contribute to the formation of soil C profiles, and the mathematical models that are used to represent them. Our main findings were: 1. The main processes that contribute to the formation of soil C profiles are root productivity and rhizodeposition, microbial decomposition, advective processes such as liquid phase transport, and diffusive processes such as bioturbation and cryoturbation. 2. These processes can be expressed in models under the general paradigm of the advection-diffusion-reaction equation, with most previously proposed models being a special case of this general paradigm. 3. Advective and diffusive processes seem to be of secondary importance in explaining the shape of vertical soil C profiles. The difference between vertical carbon inputs and decomposition seems to play a primary role in explaining the decline of soil C with depth. 4. The transit time of C is only a few years to decades in most soils, which implies that promoting the addition of new C inputs to soils would only contribute to climate change mitigation in the short term (years to decades). Carbon sequestration at longer timescales is only possible in slow cycling systems such as tundra and boreal forest soils, but primary production is relatively low in these regions.

Although soils store large quantities of C in the subsoil and this carbon is hundreds to thousands of years old, our review suggest that new carbon that enters the soil is cycled quickly by the activity of microorganisms with relatively fast transit times. Therefore, promoting new C inputs to subsoil may not have a significant contribution to climate change mitigation as it could be inferred from carbon stocks and ages in the subsoil alone. Conservation of existing subsoil C stocks seems to be a more relevant and important aspect because the timescales required to form existing soil C stocks were on the order of centuries to millenia and there are important risks that through land use change, or non-sustainable agricultural practices, important portions of these existing stocks may be lost quickly.

Acknowledgements

CAS would like to acknowledge financial support provided by the Faculty of Forest Sciences at the Swedish University of Agricultural Sciences, and the Max Planck Society. SvF received funding from the International Max Planck Research School for Global Biogeochemical Cycles (IMPRS-gBGC). This study has also received funding from the European Unions' Horizon 2020 research and innovation programme under grant agreement No. 862695 EJP SOIL.

Data availability and reproducibility of results

All code and data required to reproduce the results of this manuscript is available at <https://github.com/MPIBGC-TEE/subsoilCseq>. Upon acceptance, all files will be archived in Zenodo with a corresponding digital object identifier.

References

Ahrens, B., Braakhekke, M. C., Guggenberger, G., Schrumpf, M., and Reichstein, M. (2015). Contribution of sorption, DOC transport and microbial interactions to the ^{14}C age of a soil organic carbon profile: Insights from a calibrated process model. *Soil Biology and Biochemistry*, 88:390 – 402.

- 725 Ahrens, B., Guggenberger, G., Rethemeyer, J., John, S., Marschner, B., Heinze, S., Angst, G., Mueller,
726 C. W., Kögel-Knabner, I., Leuschner, C., Hertel, D., Bachmann, J., Reichstein, M., and Schrumpf,
727 M. (2020). Combination of energy limitation and sorption capacity explains 14c depth gradients.
728 *Soil Biology and Biochemistry*, 148:107912.
- 729 Alcántara, V., Don, A., Well, R., and Nieder, R. (2016). Deep ploughing increases agricultural soil
730 organic matter stocks. *Global Change Biology*, 22(8):2939–2956.
- 731 Allison, S. D., Wallenstein, M. D., and Bradford, M. A. (2010). Soil-carbon response to warming
732 dependent on microbial physiology. *Nature Geosci*, 3(5):336–340. 10.1038/ngeo846.
- 733 Anderson, D. H. (2013). *Compartmental modeling and tracer kinetics*, volume 50. Springer Science &
734 Business Media.
- 735 Arndt, S., Jørgensen, B. B., LaRowe, D. E., Middelburg, J. J., Pancost, R. D., and Regnier, P. (2013).
736 Quantifying the degradation of organic matter in marine sediments: A review and synthesis. *Earth-*
737 *Science Reviews*, 123(0):53–86.
- 738 Baisden, W. and Parfitt, R. (2007). Bomb 14C enrichment indicates decadal C pool in deep soil?
739 *Biogeochemistry*, 85(1):59–68.
- 740 Baisden, W. T., Amundson, R., Brenner, D. L., Cook, A. C., Kendall, C., and Harden, J. W. (2002).
741 A multiisotope c and n modeling analysis of soil organic matter turnover and transport as a func-
742 tion of soil depth in a california annual grassland soil chronosequence. *Global Biogeochem. Cycles*,
743 16(4):1135.
- 744 Balesdent, J., Basile-Doelsch, I., Chadoeuf, J., Cornu, S., Derrien, D., Fekiacova, Z., and Hatté, C.
745 (2018). Atmosphere–soil carbon transfer as a function of soil depth. *Nature*, 559(7715):599–602.
- 746 Beck, H. E., Zimmermann, N. E., McVicar, T. R., Vergopolan, N., Berg, A., and Wood, E. F. (2018).
747 Present and future köppen-geiger climate classification maps at 1-km resolution. *Scientific Data*,
748 5(1):180214.
- 749 Beer, C., Knoblauch, C., Hoyt, A. M., Hugelius, G., Palmtag, J., Mueller, C. W., and Trumbore,
750 S. (2022). Vertical pattern of organic matter decomposability in cryoturbated permafrost-affected
751 soils. *Environmental Research Letters*, 17(10):104023.
- 752 Bishop, T., McBratney, A., and Laslett, G. (1999). Modelling soil attribute depth functions with
753 equal-area quadratic smoothing splines. *Geoderma*, 91(1):27–45.
- 754 Bockheim, J. G. (2007). Importance of cryoturbation in redistributing organic carbon in permafrost-
755 affected soils. *Soil Science Society of America Journal*, 71(4):1335–1342.
- 756 Bolin, B. and Rodhe, H. (1973). A note on the concepts of age distribution and transit time in natural
757 reservoirs. *Tellus*, 25(1):58–62.
- 758 Bolinder, M., Janzen, H., Gregorich, E., Angers, D., and VandenBygaart, A. (2007). An approach
759 for estimating net primary productivity and annual carbon inputs to soil for common agricultural
760 crops in canada. *Agriculture, Ecosystems & Environment*, 118(1):29–42.
- 761 Bolinder, M. A., Crotty, F., Elsen, A., Frac, M., Kismányoky, T., Lipiec, J., Tits, M., Tóth, Z., and
762 Kätterer, T. (2020). The effect of crop residues, cover crops, manures and nitrogen fertilization on
763 soil organic carbon changes in agroecosystems: a synthesis of reviews. *Mitigation and Adaptation*
764 *Strategies for Global Change*, 25(6):929–952.
- 765 Börjesson, G., Bolinder, M. A., Kirchmann, H., and Kätterer, T. (2018). Organic carbon stocks in
766 topsoil and subsoil in long-term ley and cereal monoculture rotations. *Biology and Fertility of Soils*,
767 54(4):549–558.

- 768 Bosatta, E. and Ågren, G. I. (1996). Theoretical analyses of carbon and nutrient dynamics in soil
769 profiles. *Soil Biology and Biochemistry*, 28(10–11):1523 – 1531.
- 770 Boudreau, B. P. (1986a). Mathematics of tracer mixing in sediments; i, spatially-dependent, diffusive
771 mixing. *American Journal of Science*, 286(3):161–198.
- 772 Boudreau, B. P. (1986b). Mathematics of tracer mixing in sediments; ii, nonlocal mixing and biological
773 conveyor-belt phenomena. *American Journal of Science*, 286(3):199–238.
- 774 Boudreau, B. P. (1989). The diffusion and telegraph equations in diagenetic modelling. *Geochimica
775 et Cosmochimica Acta*, 53(8):1857–1866.
- 776 Braakhekke, M. C., Beer, C., Hoosbeek, M. R., Reichstein, M., Kruijt, B., Schrumpf, M., and Kabat, P.
777 (2011). Somprof: A vertically explicit soil organic matter model. *Ecological Modelling*, 222(10):1712–
778 1730.
- 779 Braakhekke, M. C., Wutzler, T., Beer, C., Kattge, J., Schrumpf, M., Ahrens, B., Schöning, I., Hoos-
780 beek, M. R., Kruijt, B., Kabat, P., and Reichstein, M. (2013). Modeling the vertical soil organic
781 matter profile using bayesian parameter estimation. *Biogeosciences*, 10(1):399–420.
- 782 Brovelli, A., Batlle-Aguilar, J., and Barry, D. (2012). Analysis of carbon and nitrogen dynamics in
783 riparian soils: Model development. *Science of The Total Environment*, 429:231–245. Special Section
784 - Arsenic in Latin America, An Unrevealed Continent: Occurrence, Health Effects and Mitigation.
- 785 Bruun, S., Christensen, B. T., Thomsen, I. K., Jensen, E. S., and Jensen, L. S. (2007). Modeling
786 vertical movement of organic matter in a soil incubated for 41 years with ¹⁴C labeled straw. *Soil
787 Biology and Biochemistry*, 39(1):368 – 371.
- 788 Bunzl, K. (2002). Transport of fallout radiocesium in the soil by bioturbation: a random walk model
789 and application to a forest soil with a high abundance of earthworms. *Science of The Total Envi-
790 ronment*, 293(1):191–200.
- 791 Button, E. S., Pett-Ridge, J., Murphy, D. V., Kuzyakov, Y., Chadwick, D. R., and Jones, D. L. (2022).
792 Deep-c storage: Biological, chemical and physical strategies to enhance carbon stocks in agricultural
793 subsoils. *Soil Biology and Biochemistry*, 170:108697.
- 794 Carter, M. and Gregorich, E. (2010). Carbon and nitrogen storage by deep-rooted tall fescue (*Iolium
795 arundinaceum*) in the surface and subsurface soil of a fine sandy loam in eastern canada. *Agriculture,
796 Ecosystems & Environment*, 136(1):125–132.
- 797 Chabbi, A., Kögel-Knabner, I., and Rumpel, C. (2009). Stabilised carbon in subsoil horizons is located
798 in spatially distinct parts of the soil profile. *Soil Biology and Biochemistry*, 41(2):256–261.
- 799 Chen, S., Martin, M. P., Saby, N. P., Walter, C., Angers, D. A., and Arrouays, D. (2018). Fine
800 resolution map of top- and subsoil carbon sequestration potential in france. *Science of The Total
801 Environment*, 630:389–400.
- 802 Chenu, C., Angers, D. A., Barré, P., Derrien, D., Arrouays, D., and Balesdent, J. (2019). Increasing
803 organic stocks in agricultural soils: Knowledge gaps and potential innovations. *Soil and Tillage
804 Research*, 188:41–52. Soil Carbon and Climate Change: the 4 per Mille Initiative.
- 805 Choi, J., Francois-Carcaillet, F., and Boudreau, B. P. (2002). Lattice-automaton bioturbation simu-
806 lator (labs): implementation for small deposit feeders. *Computers & Geosciences*, 28(2):213–222.
- 807 Collins, H., Smith, J., Fransen, S., Alva, A., Kruger, C., and Granatstein, D. (2010). Carbon se-
808 questration under irrigated switchgrass (*panicum virgatum* l.) production. *Soil Science Society of
809 America Journal*, 74(6):2049–2058.

- 810 Cotrufo, M. F. and Lavallee, J. M. (2022). Soil organic matter formation, persistence, and functioning:
811 A synthesis of current understanding to inform its conservation and regeneration. *Advances in*
812 *Agronomy*, 172:1–66.
- 813 Crow, S., Reeves, M., Schubert, O., and Sierra, C. (2015). Optimization of method to quantify soil
814 organic matter dynamics and carbon sequestration potential in volcanic ash soils. *Biogeochemistry*,
815 123(1-2):27–47.
- 816 Crow, S. E. and Sierra, C. A. (2022). The climate benefit of sequestration in soils for warming
817 mitigation. *Biogeochemistry*, 161:71–84.
- 818 Dal Ferro, N., Piccoli, I., Berti, A., Polese, R., and Morari, F. (2020). Organic carbon storage potential
819 in deep agricultural soil layers: Evidence from long-term experiments in northeast Italy. *Agriculture,*
820 *Ecosystems & Environment*, 300:106967.
- 821 Don, A., Rödenbeck, C., and Gleixner, G. (2013). Unexpected control of soil carbon turnover by soil
822 carbon concentration. *Environmental Chemistry Letters*, pages 1–7.
- 823 Dörr, H. and Münnich, K. O. (1989). Downward movement of soil organic matter and its influence on
824 trace-element transport (^{210}Pb , ^{137}Cs) in the soil. *Radiocarbon*, 31(3):655–663.
- 825 Elzein, A. and Balesdent, J. (1995). Mechanistic simulation of vertical distribution of carbon concen-
826 trations and residence times in soils. *Soil Sci. Soc. Am. J.*, 59(5):1328–1335.
- 827 Eusterhues, K., Rumpel, C., Kleber, M., and Kögel-Knabner, I. (2003). Stabilisation of soil organic
828 matter by interactions with minerals as revealed by mineral dissolution and oxidative degradation.
829 *Organic Geochemistry*, 34(12):1591–1600.
- 830 Fan, J., McConkey, B., Wang, H., and Janzen, H. (2016). Root distribution by depth for temperate
831 agricultural crops. *Field Crops Research*, 189:68–74.
- 832 Feng, X., Peterson, J. C., Quideau, S. A., Virginia, R. A., Graham, R. C., Sonder, L. J., and Chadwick,
833 O. A. (1999). Distribution, accumulation, and fluxes of soil carbon in four monoculture lysimeters
834 at San Dimas experimental forest, California. *Geochimica et Cosmochimica Acta*, 63(9):1319–1333.
- 835 Fey, M. V. and Schaetzl, R. J. (2017). Pedoturbation. In *International Encyclopedia of Geography*,
836 pages 1–11. John Wiley & Sons, Ltd.
- 837 Finke, P. A. (2012). Modeling the genesis of Luvisols as a function of topographic position in loess
838 parent material. *Quaternary International*, 265:3–17. Paleosols in landscapes of the past and present.
- 839 Freier, K. P., GLASER, B., and ZECH, W. (2010). Mathematical modeling of soil carbon turnover
840 in natural Podocarpus forest and eucalyptus plantation in Ethiopia using compound specific $\delta^{13}\text{C}$
841 analysis. *Global Change Biology*, 16(5):1487–1502.
- 842 Gale, M. R. and Grigal, D. F. (1987). Vertical root distributions of northern tree species in relation
843 to successional status. *Canadian Journal of Forest Research*, 17(8):829–834.
- 844 Georgiou, K., Jackson, R. B., Vinduřková, O., Abramoff, R. Z., Ahlström, A., Feng, W., Harden,
845 J. W., Pellegrini, A. F. A., Polley, H. W., Soong, J. L., Riley, W. J., and Torn, M. S. (2022). Global
846 stocks and capacity of mineral-associated soil organic carbon. *Nature Communications*, 13(1):3797.
- 847 Gill, R. A. and Jackson, R. B. (2000). Global patterns of root turnover for terrestrial ecosystems. *New*
848 *Phytologist*, 147(1):13–31.
- 849 Gjettermann, B., Styczen, M., Hansen, H. C. B., Vinther, F. P., and Hansen, S. (2008). Challenges in
850 modelling dissolved organic matter dynamics in agricultural soil using daisy. *Soil Biology and Bio-*
851 *chemistry*, 40(6):1506–1518. Special Section: Functional Microbial Ecology: Molecular Approaches
852 to Microbial Ecology and Microbial Habitats.

853 Gleixner, G. (2013). Soil organic matter dynamics: a biological perspective derived from the use of
854 compound-specific isotopes studies. *Ecological Research*, 28(5):683–695.

855 Grant, R., Juma, N., and McGill, W. (1993). Simulation of carbon and nitrogen transformations in
856 soil: Mineralization. *Soil Biology and Biochemistry*, 25(10):1317–1329.

857 Guan, X.-K., Turner, N. C., Song, L., Gu, Y.-J., Wang, T.-C., and Li, F.-M. (2016). Soil carbon
858 sequestration by three perennial legume pastures is greater in deeper soil layers than in the surface
859 soil. *Biogeosciences*, 13(2):527–534.

860 Guenet, B., Eglin, T., Vasilyeva, N., Peylin, P., Ciais, P., and Chenu, C. (2013). The relative im-
861 portance of decomposition and transport mechanisms in accounting for soil organic carbon profiles.
862 *Biogeosciences*, 10(4):2379–2392.

863 Guo, L. B. and Gifford, R. M. (2002). Soil carbon stocks and land use change: a meta analysis. *Global*
864 *Change Biology*, 8(4):345–360.

865 Guo, X., Mao, X., Yu, W., Xiao, L., Wang, M., Zhang, S., Zheng, J., Zhou, H., Luo, L., Chang, J.,
866 Shi, Z., and Luo, Z. (2023). A field incubation approach to evaluate the depth dependence of soil
867 biogeochemical responses to climate change. *Global Change Biology*, 29(3):909–920.

868 Hansen, S., Jensen, H. E., Nielsen, N. E., and Svendsen, H. (1991). Simulation of nitrogen dynamics
869 and biomass production in winter wheat using the danish simulation model daisy. *Fertilizer research*,
870 27(2):245–259.

871 He, Y., Trumbore, S. E., Torn, M. S., Harden, J. W., Vaughn, L. J. S., Allison, S. D., and Randerson,
872 J. T. (2016). Radiocarbon constraints imply reduced carbon uptake by soils during the 21st century.
873 *Science*, 353(6306):1419–1424.

874 Heckman, K., Hicks Pries, C. E., Lawrence, C. R., Rasmussen, C., Crow, S. E., Hoyt, A. M., von
875 Fromm, S. F., Shi, Z., Stoner, S., McGrath, C., Beem-Miller, J., Berhe, A. A., Blankinship, J. C.,
876 Keiluweit, M., Marín-Spiotta, E., Monroe, J. G., Plante, A. F., Schimel, J., Sierra, C. A., Thompson,
877 A., and Wagai, R. (2022). Beyond bulk: Density fractions explain heterogeneity in global soil carbon
878 abundance and persistence. *Global Change Biology*, 28(3):1178–1196.

879 Hicks Pries, C., Ryals, R., Zhu, B., Min, K., Cooper, A., Goldsmith, S., Pett-Ridge, J., Torn, M., and
880 Asefaw Berhe, A. (2023). The deep soil organic carbon response to global change. *Annual Review*
881 *of Ecology, Evolution, and Systematics*, 54(1):null.

882 Hilinski, T. E. (2001). Implementation of exponential depth distribution of organic carbon in the
883 century model.

884 Hinzmann, M., Ittner, S., Kiresiewa, Z., and Gerdes, H. (2021). An acceptance analysis of subsoil
885 amelioration amongst agricultural actors in two regions in germany. *Frontiers in Agronomy*, 3.

886 Hole, F. D. (1961). A classification of pedoturbations and some other processes and factors of soil
887 formation in relation to isotropism and anisotropism. *Soil Science*, 91:375–377.

888 Huang, Y., Lu, X., Shi, Z., Lawrence, D., Koven, C. D., Xia, J., Du, Z., Kluzek, E., and Luo, Y.
889 (2018). Matrix approach to land carbon cycle modeling: A case study with the community land
890 model. *Global Change Biology*, 24(3):1394–1404.

891 Jackson, R., Canadell, J., Ehleringer, J., Mooney, H., Sala, O., and Schulze, E. (1996). A global
892 analysis of root distributions for terrestrial biomes. *Oecologia*, 10:389–411.

893 Jackson, R., Mooney, H., and Schulze, E.-D. (1997). A global budget for fine root biomass, surface
894 area, and nutrient contents. *Proceedings of the National Academy of Sciences USA*, 94:7362–7366.

895 Jenkinson, D. S. and Coleman, K. (2008). The turnover of organic carbon in subsoils. part 2. modelling
896 carbon turnover. *European Journal of Soil Science*, 59(2):400–413.

- 897 Jobbágy, E. and Jackson, R. (2000). The vertical distribution of soil organic carbon and its relation
898 to climate and vegetation. *Ecological Applications*, pages 10(2):423–436.
- 899 Johnson, D. L., Watson-Stegner, D., Johnson, D. N., and Schaetzl, R. J. (1987). Proisotropic and
900 proanisotropic processes of pedoturbation. *Soil Science*, 143:278–292.
- 901 Jordan, C. F. and Escalante, G. (1980). Root productivity in an amazonian rain forest. *Ecology*,
902 61(1):14–18. 0012-9658 Article type: Full Length Article / Full publication date: Feb., 1980
903 (198002). / Languages: EN / Copyright 1980 Ecological Society of America.
- 904 Kaiser, K. and Kalbitz, K. (2012). Cycling downwards – dissolved organic matter in soils. *Soil Biology
905 and Biochemistry*, 52:29–32.
- 906 Kalbitz, K. and Kaiser, K. (2008). Contribution of dissolved organic matter to carbon storage in forest
907 mineral soils. *Journal of Plant Nutrition and Soil Science*, 171(1):52–60.
- 908 Kaste, J. M., Heimsath, A. M., and Bostick, B. C. (2007). Short-term soil mixing quantified with
909 fallout radionuclides. *Geology*, 35(3):243–246.
- 910 Kätterer, T., Börjesson, G., and Kirchmann, H. (2014). Changes in organic carbon in topsoil and sub-
911 soil and microbial community composition caused by repeated additions of organic amendments and
912 n fertilisation in a long-term field experiment in sweden. *Agriculture, Ecosystems & Environment*,
913 189:110–118.
- 914 Kautz, T., Amelung, W., Ewert, F., Gaiser, T., Horn, R., Jahn, R., Javaux, M., Kemna, A., Kuzyakov,
915 Y., Munch, J.-C., Pätzold, S., Peth, S., Scherer, H. W., Schloter, M., Schneider, H., Vanderborght,
916 J., Vetterlein, D., Walter, A., Wiesenberger, G. L., and Köpke, U. (2013). Nutrient acquisition from
917 arable subsoils in temperate climates: A review. *Soil Biology and Biochemistry*, 57:1003–1022.
- 918 Kell, D. B. (2011). Breeding crop plants with deep roots: their role in sustainable carbon, nutrient
919 and water sequestration. *Annals of Botany*, 108(3):407–418.
- 920 Keyvanshokouhi, S., Cornu, S., Lafolie, F., Balesdent, J., Guenet, B., Moitrier, N., Moitrier, N.,
921 Nougier, C., and Finke, P. (2019). Effects of soil process formalisms and forcing factors on simulated
922 organic carbon depth-distributions in soils. *Science of The Total Environment*, 652:523–537.
- 923 Kindler, R., SIEMENS, J., KAISER, K., WALMSLEY, D. C., BERNHOFER, C., BUCHMANN, N.,
924 CELLIER, P., EUGSTER, W., GLEIXNER, G., GRÜNWALD, T., HEIM, A., IBROM, A., JONES,
925 S. K., JONES, M., KLUMPP, K., KUTSCH, W., LARSEN, K. S., LEHUGER, S., LOUBET, B.,
926 MCKENZIE, R., MOORS, E., OSBORNE, B., PILEGAARD, K., REBMANN, C., SAUNDERS,
927 M., SCHMIDT, M. W. I., SCHRUMPF, M., SEYFFERTH, J., SKIBA, U., SOUSSANA, J.-F.,
928 SUTTON, M. A., TEFS, C., VOWINCKEL, B., ZEEMAN, M. J., and KAUPENJOHANN, M.
929 (2011). Dissolved carbon leaching from soil is a crucial component of the net ecosystem carbon
930 balance. *Global Change Biology*, 17(2):1167–1185.
- 931 Kirchmann, H., Schön, M., Börjesson, G., Hamnér, K., and Kätterer, T. (2013). Properties of soils in
932 the swedish long-term fertility experiments: Vii. changes in topsoil and upper subsoil at örja and
933 fors after 50 years of nitrogen fertilization and manure application. *Acta Agriculturae Scandinavica*,
934 *Section B — Soil & Plant Science*, 63(1):25–36.
- 935 Kirkby, M. J. (1977). Soil development models as a component of slope models. *Earth Surface
936 Processes*, 2(2-3):203–230.
- 937 Koven, C., Friedlingstein, P., Ciais, P., Khvorostyanov, D., Krinner, G., and Tarnocai, C. (2009). On
938 the formation of high-latitude soil carbon stocks: Effects of cryoturbation and insulation by organic
939 matter in a land surface model. *Geophysical Research Letters*, 36(21).

- 940 Koven, C. D., Riley, W. J., Subin, Z. M., Tang, J. Y., Torn, M. S., Collins, W. D., Bonan, G. B.,
941 Lawrence, D. M., and Swenson, S. C. (2013). The effect of vertically resolved soil biogeochemistry
942 and alternate soil c and n models on c dynamics of clm4. *Biogeosciences*, 10(11):7109–7131.
- 943 Lanczos, C. (1996). *Linear Differential Operators*. Society for Industrial and Applied Mathematics.
- 944 Lawrence, C. R., Beem-Miller, J., Hoyt, A. M., Monroe, G., Sierra, C. A., Stoner, S., Heckman, K.,
945 Blankinship, J. C., Crow, S. E., McNicol, G., Trumbore, S., Levine, P. A., Vinduřková, O., Todd-
946 Brown, K., Rasmussen, C., Hicks Pries, C. E., Schädel, C., McFarlane, K., Doetterl, S., Hatté, C.,
947 He, Y., Treat, C., Harden, J. W., Torn, M. S., Estop-Aragonés, C., Asefaw Berhe, A., Keiluweit,
948 M., Della Rosa Kuhnen, A., Marin-Spiotta, E., Plante, A. F., Thompson, A., Shi, Z., Schimel,
949 J. P., Vaughn, L. J. S., von Fromm, S. F., and Wagai, R. (2020). An open-source database for the
950 synthesis of soil radiocarbon data: International Soil Radiocarbon Database (ISRaD) version 1.0.
951 *Earth System Science Data*, 12(1):61–76.
- 952 LeVeque, R. J. (1990). *Numerical Methods for Conservation Laws*. Birkhäuser Basel.
- 953 LeVeque, R. J. (2007). *Finite difference methods for ordinary and partial differential equations: steady-
954 state and time-dependent problems*. Society for Industrial and Applied Mathematics, Philadelphia,
955 PA. 2007061732 Randall J. LeVeque. ill. ; 26 cm. Includes bibliographical references (p. 329-335)
956 and index.
- 957 Li, C., Frolking, S., and Frolking, T. A. (1992). A model of nitrous oxide evolution from soil driven by
958 rainfall events: 1. model structure and sensitivity. *Journal of Geophysical Research: Atmospheres*,
959 97(D9):9759–9776.
- 960 Liang, J., Zhou, Z., Huo, C., Shi, Z., Cole, J. R., Huang, L., Konstantinidis, K. T., Li, X., Liu, B.,
961 Luo, Z., Penton, C. R., Schuur, E. A. G., Tiedje, J. M., Wang, Y.-P., Wu, L., Xia, J., Zhou, J.,
962 and Luo, Y. (2018). More replenishment than priming loss of soil organic carbon with additional
963 carbon input. *Nature Communications*, 9(1):3175.
- 964 Liu, F., Wang, D., Zhang, B., and Huang, J. (2021). Concentration and biodegradability of dis-
965 solved organic carbon derived from soils: A global perspective. *Science of The Total Environment*,
966 754:142378.
- 967 Lorenz, K. and Lal, R. (2005). The depth distribution of soil organic carbon in relation to land use and
968 management and the potential of carbon sequestration in subsoil horizons. *Advances in Agronomy*,
969 88:35–66.
- 970 Lu, X., Wang, Y.-P., Luo, Y., and Jiang, L. (2018). Ecosystem carbon transit versus turnover
971 times in response to climate warming and rising atmospheric CO₂ concentration. *Biogeosciences*,
972 15(21):6559–6572.
- 973 Luo, Z., Luo, Y., Wang, G., Xia, J., and Peng, C. (2020). Warming-induced global soil carbon loss
974 attenuated by downward carbon movement. *Global Change Biology*, 26(12):7242–7254.
- 975 Luo, Z., Wang, E., and Sun, O. J. (2010). Can no-tillage stimulate carbon sequestration in agricultural
976 soils? a meta-analysis of paired experiments. *Agriculture, Ecosystems & Environment*, 139(1):224–
977 231.
- 978 Manzoni, S., Katul, G. G., and Porporato, A. (2009). Analysis of soil carbon transit times and age
979 distributions using network theories. *J. Geophys. Res.*, 114.
- 980 Manzoni, S. and Porporato, A. (2009). Soil carbon and nitrogen mineralization: Theory and models
981 across scales. *Soil Biology and Biochemistry*, 41(7):1355 – 1379.
- 982 Marin-Spiotta, E., Chadwick, O. A., Kramer, M., and Carbone, M. S. (2011). Carbon delivery to deep
983 mineral horizons in hawaiian rain forest soils. *Journal of Geophysical Research: Biogeosciences*,
984 116(G3).

- Mary, B., Clivot, H., Blaszczyk, N., Labreuche, J., and Ferchaud, F. (2020). Soil carbon storage and mineralization rates are affected by carbon inputs rather than physical disturbance: Evidence from a 47-year tillage experiment. *Agriculture, Ecosystems & Environment*, 299:106972.
- Mathieu, J. A., Hatté, C., Balesdent, J., and Parent, É. (2015). Deep soil carbon dynamics are driven more by soil type than by climate: a worldwide meta-analysis of radiocarbon profiles. *Global Change Biology*, 21(11):4278–4292.
- Menichetti, L., Ekblad, A., and Kätterer, T. (2015). Contribution of roots and amendments to soil carbon accumulation within the soil profile in a long-term field experiment in sweden. *Agriculture, Ecosystems & Environment*, 200:79–87.
- Metzler, H. and Sierra, C. A. (2018). Linear autonomous compartmental models as continuous-time Markov chains: Transit-time and age distributions. *Mathematical Geosciences*, 50(1):1–34.
- Metzler, H., Zhu, Q., Riley, W., Hoyt, A., Müller, M., and Sierra, C. A. (2020). Mathematical reconstruction of land carbon models from their numerical output: Computing soil radiocarbon from c dynamics. *Journal of Advances in Modeling Earth Systems*, 12(1):e2019MS001776. e2019MS001776 10.1029/2019MS001776.
- Meysman, F. J., Boudreau, B. P., and Middelburg, J. J. (2005). Modeling reactive transport in sediments subject to bioturbation and compaction. *Geochimica et Cosmochimica Acta*, 69(14):3601–3617.
- Meysman, F. J., Malyuga, V. S., Boudreau, B. P., and Middelburg, J. J. (2008). A generalized stochastic approach to particle dispersal in soils and sediments. *Geochimica et Cosmochimica Acta*, 72(14):3460–3478.
- Meysman, F. J. R., Boudreau, B. P., and Middelburg, J. J. (2003). Relations between local, nonlocal, discrete and continuous models of bioturbation. *Journal of Marine Research*, 61:391–410.
- Meysman, F. J. R., Boudreau, B. P., and Middelburg, J. J. (2010). When and why does bioturbation lead to diffusive mixing. *Journal of Marine Research*, 68:881–920.
- Michalzik, B., Kalbitz, K., Park, J. H., Solinger, S., and Matzner, E. (2001). Fluxes and concentrations of dissolved organic carbon and nitrogen –a synthesis for temperate forests. *Biogeochemistry*, 52(2):173–205.
- Michalzik, B., Tipping, E., Mulder, J., Lancho, J. F. G., Matzner, E., Bryant, C. L., Clarke, N., Lofts, S., and Esteban, M. A. V. (2003). Modelling the production and transport of dissolved organic carbon in forest soils. *Biogeochemistry*, 66(3):241–264.
- Morari, F., Berti, A., Dal Ferro, N., and Piccoli, I. (2019). *Deep Carbon Sequestration in Cropping Systems*, pages 33–65. Springer International Publishing, Cham.
- Mosier, S., Córdova, S. C., and Robertson, G. P. (2021). Restoring soil fertility on degraded lands to meet food, fuel, and climate security needs via perennialization. *Frontiers in Sustainable Food Systems*, 5.
- Moyano, F. E., Manzoni, S., and Chenu, C. (2013). Responses of soil heterotrophic respiration to moisture availability: An exploration of processes and models. *Soil Biology and Biochemistry*, 59(0):72 – 85.
- Müller-Lemans, H. and van Dorp, F. (1996). Bioturbation as a mechanism for radionuclide transport in soil: Relevance of earthworms. *Journal of Environmental Radioactivity*, 31(1):7–20.
- Nakane, K. and Shinozaki, K. (1978). A mathematical model of the behavior and vertical distribution of organic carbon in forest soils. *JAPANESE JOURNAL OF ECOLOGY*, 28(2):111–122.

- 1028 Neff, J. C. and Asner, G. P. (2001). Dissolved organic carbon in terrestrial ecosystems: Synthesis and
1029 a model. *Ecosystems*, 4(1):29–48.
- 1030 O’Brien, B. and Stout, J. (1978). Movement and turnover of soil organic matter as indicated by carbon
1031 isotope measurements. *Soil Biology and Biochemistry*, 10(4):309 – 317.
- 1032 Ota, M., Nagai, H., and Koarashi, J. (2013). Root and dissolved organic carbon controls on subsur-
1033 face soil carbon dynamics: A model approach. *Journal of Geophysical Research: Biogeosciences*,
1034 118(4):1646–1659.
- 1035 Paustian, K., Lehmann, J., Ogle, S., Reay, D., Robertson, G. P., and Smith, P. (2016). Climate-smart
1036 soils. *Nature*, 532(7597):49–57.
- 1037 Persson, T., Karlsson, P. S., Seyferth, U., Sjöberg, R. M., and Rudebeck, A. (2000). *Carbon Mineral-*
1038 *isation in European Forest Soils*, pages 257–275. Springer Berlin Heidelberg, Berlin, Heidelberg.
- 1039 Poeplau, C. and Don, A. (2013). Sensitivity of soil organic carbon stocks and fractions to different
1040 land-use changes across europe. *Geoderma*, 192:189–201.
- 1041 Ponce-Hernandez, R., Marriott, F. H. C., and Beckett, P. H. T. (1986). An improved method for
1042 reconstructing a soil profile from analyses of a small number of samples. *Journal of Soil Science*,
1043 37(3):455–467.
- 1044 Raich, J. and Nadelhoffer, K. (1989). Belowground carbon allocation in forest ecosystems: global
1045 trends. *Ecology*, 70(5):1346–1354.
- 1046 Rasmussen, C., Heckman, K., Wieder, W. R., Keiluweit, M., Lawrence, C. R., Berhe, A. A., Blank-
1047 inship, J. C., Crow, S. E., Druhan, J. L., Hicks Pries, C. E., Marin-Spiotta, E., Plante, A. F.,
1048 Schädel, C., Schimel, J. P., Sierra, C. A., Thompson, A., and Wagai, R. (2018). Beyond clay:
1049 towards an improved set of variables for predicting soil organic matter content. *Biogeochemistry*,
1050 137(3):297–306.
- 1051 Rosenbloom, N. A., Doney, S. C., and Schimel, D. S. (2001). Geomorphic evolution of soil texture
1052 and organic matter in eroding landscapes. *Global Biogeochemical Cycles*, 15(2):365–381.
- 1053 Roth, V.-N., Lange, M., Simon, C., Hertkorn, N., Bucher, S., Goodall, T., Griffiths, R. I., Mellado-
1054 Vázquez, P. G., Mommer, L., Oram, N. J., Weigelt, A., Dittmar, T., and Gleixner, G. (2019).
1055 Persistence of dissolved organic matter explained by molecular changes during its passage through
1056 soil. *Nature Geoscience*, 12(9):755–761.
- 1057 Rumpel, C., Chabbi, A., and Marschner, B. (2012). *Carbon Storage and Sequestration in Subsoil*
1058 *Horizons: Knowledge, Gaps and Potentials*, pages 445–464. Springer Netherlands, Dordrecht.
- 1059 Rumpel, C. and Kögel-Knabner, I. (2011). Deep soil organic matter—a key but poorly understood
1060 component of terrestrial c cycle. *Plant and Soil*, 338(1):143–158.
- 1061 Salvador-Blanes, S., Minasny, B., and McBratney, A. B. (2007). Modelling long-term in situ soil profile
1062 evolution: application to the genesis of soil profiles containing stone layers. *European Journal of*
1063 *Soil Science*, 58(6):1535–1548.
- 1064 Sanderman, J., Hengl, T., and Fiske, G. J. (2017). Soil carbon debt of 12,000 years of human land
1065 use. *Proceedings of the National Academy of Sciences*, 114(36):9575–9580.
- 1066 Sarmiento, J. and Gruber, N. (2006). *Ocean Biogeochemical Dynamics*. Princeton University Press,
1067 Princeton.
- 1068 Schaetzl, R. J., Burns, S. F., Small, T. W., and Johnson, D. L. (1990). Tree uprooting: Review of
1069 types and patterns of soil disturbance. *Physical Geography*, 11(3):277–291.

1070 Scheibe, A., Sierra, C. A., and Spohn, M. (2023). Recently fixed carbon fuels microbial activity several
1071 meters below the soil surface. *Biogeosciences*, 20(4):827–838.

1072 Schenk, H. and Jackson, R. (2002a). The global biogeography of roots. *Ecological Monographs*, pages
1073 72(3):311–328.

1074 Schenk, H. and Jackson, R. (2002b). Rooting depths, lateral root spreads and below-ground/above-
1075 ground allometries of plants in water limited ecosystem. *Journal of Ecology*, pages 90:480–494.

1076 Schiedung, M., Tregurtha, C. S., Beare, M. H., Thomas, S. M., and Don, A. (2019). Deep soil flipping
1077 increases carbon stocks of new zealand grasslands. *Global Change Biology*, 25(7):2296–2309.

1078 Schimel, J. P. and Weintraub, M. N. (2003). The implications of exoenzyme activity on micro-
1079 bial carbon and nitrogen limitation in soil: a theoretical model. *Soil Biology and Biochemistry*,
1080 35(4):549–563.

1081 Shi, Z., Allison, S. D., He, Y., Levine, P. A., Hoyt, A. M., Beem-Miller, J., Zhu, Q., Wieder, W. R.,
1082 Trumbore, S., and Randerson, J. T. (2020). The age distribution of global soil carbon inferred from
1083 radiocarbon measurements. *Nature Geoscience*, 13(8):555–559.

1084 Sierra, C. A., Ceballos-Núñez, V., Metzler, H., and Müller, M. (2018a). Representing and understand-
1085 ing the carbon cycle using the theory of compartmental dynamical systems. *Journal of Advances
1086 in Modeling Earth Systems*, 10(8):1729–1734.

1087 Sierra, C. A., Crow, S. E., Heimann, M., Metzler, H., and Schulze, E.-D. (2021a). The climate benefit
1088 of carbon sequestration. *Biogeosciences*, 18(3):1029–1048.

1089 Sierra, C. A., Estupinan-Suarez, L. M., and Chanca, I. (2021b). The fate and transit time of carbon
1090 in a tropical forest. *Journal of Ecology*, 109(8):2845–2855.

1091 Sierra, C. A., Hoyt, A. M., He, Y., and Trumbore, S. E. (2018b). Soil organic matter persistence as
1092 a stochastic process: Age and transit time distributions of carbon in soils. *Global Biogeochemical
1093 Cycles*, 32(10):1574–1588.

1094 Sierra, C. A. and Müller, M. (2015). A general mathematical framework for representing soil organic
1095 matter dynamics. *Ecological Monographs*, 85:505–524.

1096 Sierra, C. A., Müller, M., Metzler, H., Manzoni, S., and Trumbore, S. E. (2017). The muddle of ages,
1097 turnover, transit, and residence times in the carbon cycle. *Global Change Biology*, 23(5):1763–1773.

1098 Sierra, C. A., Trumbore, S. E., Davidson, E. A., Vicca, S., and Janssens, I. (2015). Sensitivity of
1099 decomposition rates of soil organic matter with respect to simultaneous changes in temperature and
1100 moisture. *Journal of Advances in Modeling Earth Systems*, 7(1):335–356.

1101 Slessarev, E. W., Nuccio, E. E., McFarlane, K. J., Ramon, C. E., Saha, M., Firestone, M. K., and
1102 Pett-Ridge, J. (2020). Quantifying the effects of switchgrass (*panicum virgatum*) on deep organic c
1103 stocks using natural abundance $\delta^{13}C$ in three marginal soils. *GCB Bioenergy*, 12(10):834–847.

1104 Taghizadeh-Toosi, A., Christensen, B. T., Hutchings, N. J., Vejlin, J., Kätterer, T., Glendining, M.,
1105 and Olesen, J. E. (2014). C-tool: A simple model for simulating whole-profile carbon storage in
1106 temperate agricultural soils. *Ecological Modelling*, 292:11–25.

1107 Thompson, M. V. and Randerson, J. T. (1999). Impulse response functions of terrestrial carbon
1108 cycle models: method and application. *Global Change Biology*, 5(4):371–394. 10.1046/j.1365-
1109 2486.1999.00235.x.

1110 Thorup-Kristensen, K., Halberg, N., Nicolaisen, M., Olesen, J. E., Crews, T. E., Hinsinger, P.,
1111 Kirkegaard, J., Pierret, A., and Dresbøll, D. B. (2020). Digging deeper for agricultural resources,
1112 the value of deep rooting. *Trends in Plant Science*, 25(4):406–417.

1113 Tifafi, M., Camino-Serrano, M., Hatté, C., Morras, H., Moretti, L., Barbaro, S., Cornu, S., and Guenet,
1114 B. (2018). The use of radiocarbon ^{14}C to constrain carbon dynamics in the soil module of the land
1115 surface model ORCHIDEE (SVN r5165). *Geoscientific Model Development*, 11(12):4711–4726.

1116 van Dam, D., van Breemen, N., and Veldkamp, E. (1997). Soil organic carbon dynamics: variability
1117 with depth in forested and deforested soils under pasture in costa rica. *Biogeochemistry*, 39(3):343–
1118 375.

1119 van Veen, J. A. and Paul, E. A. (1981). Organic carbon dynamics in grassland soils. 1. background
1120 information and computer simulation. *Canadian Journal of Soil Science*, 61(2):185–201.

1121 VandenBygaart, A. J., Bremer, E., McConkey, B. G., Ellert, B. H., Janzen, H. H., Angers, D. A.,
1122 Carter, M. R., Drury, C. F., Lafond, G. P., and McKenzie, R. H. (2011). Impact of sampling depth
1123 on differences in soil carbon stocks in long-term agroecosystem experiments. *Soil Science Society of
1124 America Journal*, 75(1):226–234.

1125 Wang, G., Xiao, L., Lin, Z., Zhang, Q., Guo, X., Cowie, A., Zhang, S., Wang, M., Chen, S., Zhang,
1126 G., Shi, Z., Sun, W., and Luo, Z. (2023a). Most root-derived carbon inputs do not contribute to
1127 long-term global soil carbon storage. *Science China Earth Sciences*, 66(5):1072–1086.

1128 Wang, X., Xu, X., Qiu, S., Zhao, S., and He, P. (2023b). Deep tillage enhanced soil organic carbon
1129 sequestration in china: A meta-analysis. *Journal of Cleaner Production*, 399:136686.

1130 Wang, Y.-P., Zhang, H., Ciais, P., Goll, D., Huang, Y., Wood, J. D., Ollinger, S. V., Tang, X.,
1131 and Prescher, A.-K. (2021). Microbial activity and root carbon inputs are more important than soil
1132 carbon diffusion in simulating soil carbon profiles. *Journal of Geophysical Research: Biogeosciences*,
1133 126(4):e2020JG006205. e2020JG006205 2020JG006205.

1134 Xiao, L., Wang, G., Chang, J., Chen, Y., Guo, X., Mao, X., Wang, M., Zhang, S., Shi, Z., Luo,
1135 Y., Cheng, L., Yu, K., Mo, F., and Luo, Z. (2023). Global depth distribution of belowground net
1136 primary productivity and its drivers. *Global Ecology and Biogeography*, in press.

1137 Xiao, L., Wang, G., Wang, M., Zhang, S., Sierra, C. A., Guo, X., Chang, J., Shi, Z., and Luo, Z. (2022).
1138 Younger carbon dominates global soil carbon efflux. *Global Change Biology*, 28(18):5587–5599.

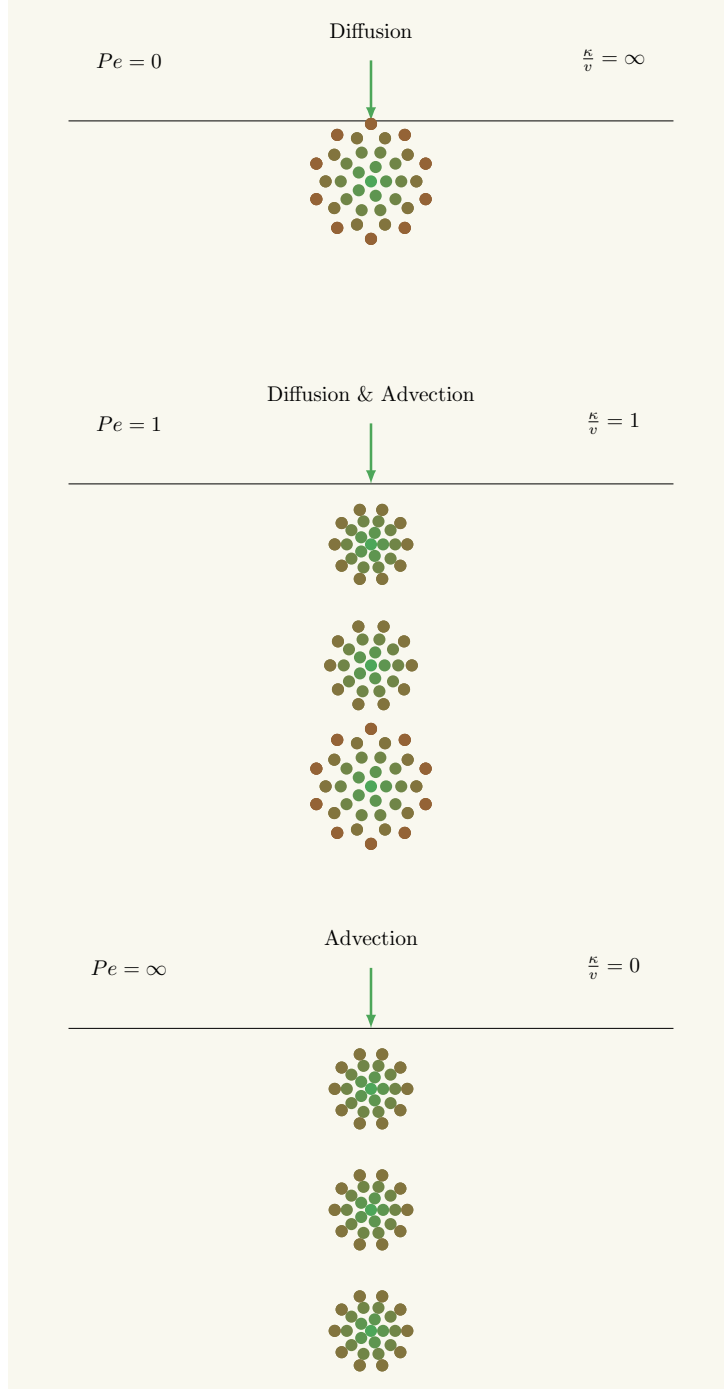


Figure 1: Schematic representation of the role of the Péclet number, which is the inverse of the κ/v ratio, on the type of vertical C transfer in a soil assuming a pulse of aboveground inputs. For a Péclet number of zero and $\kappa/v = \infty$, C entering the soil only moves due to diffusion (top); for a Péclet number and $\kappa/v = 1$, both diffusion and advection moves the carbon vertically (center); for a Péclet number of ∞ and $\kappa/v = 0$, C is only moved vertically by advective processes as in the case of DOC transport (bottom).

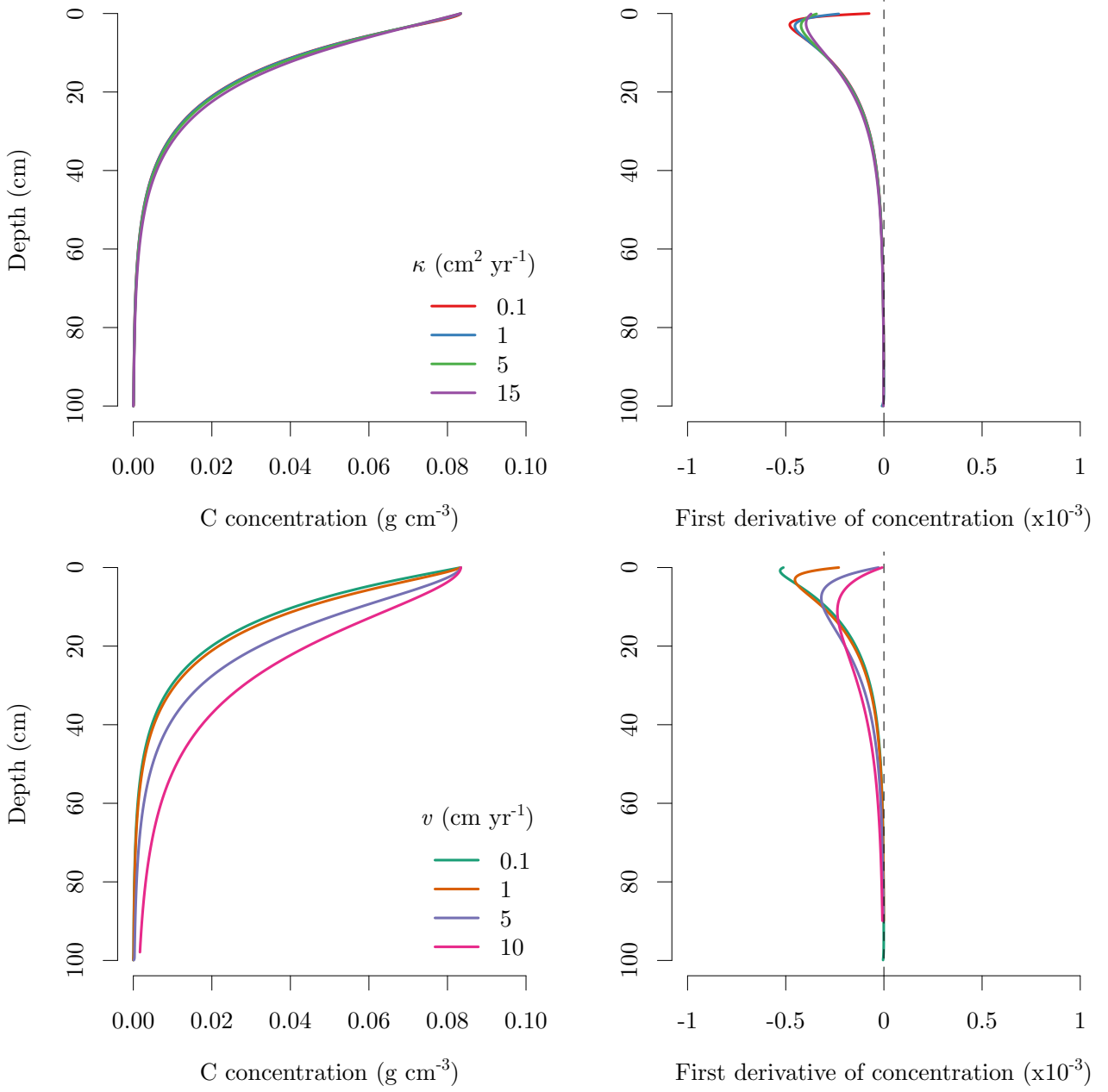


Figure 2: Numerical simulations of soil C depth profiles using the linear model with constant coefficients of equation 17. The top panels show the C concentration and the first derivative of C concentrations for different values of κ and a fixed value of $v = 1 \text{ cm yr}^{-1}$. The bottom panels show C concentrations and their first derivative for different values of v and a constant value of $\kappa = 1 \text{ cm}^2 \text{ yr}^{-1}$.

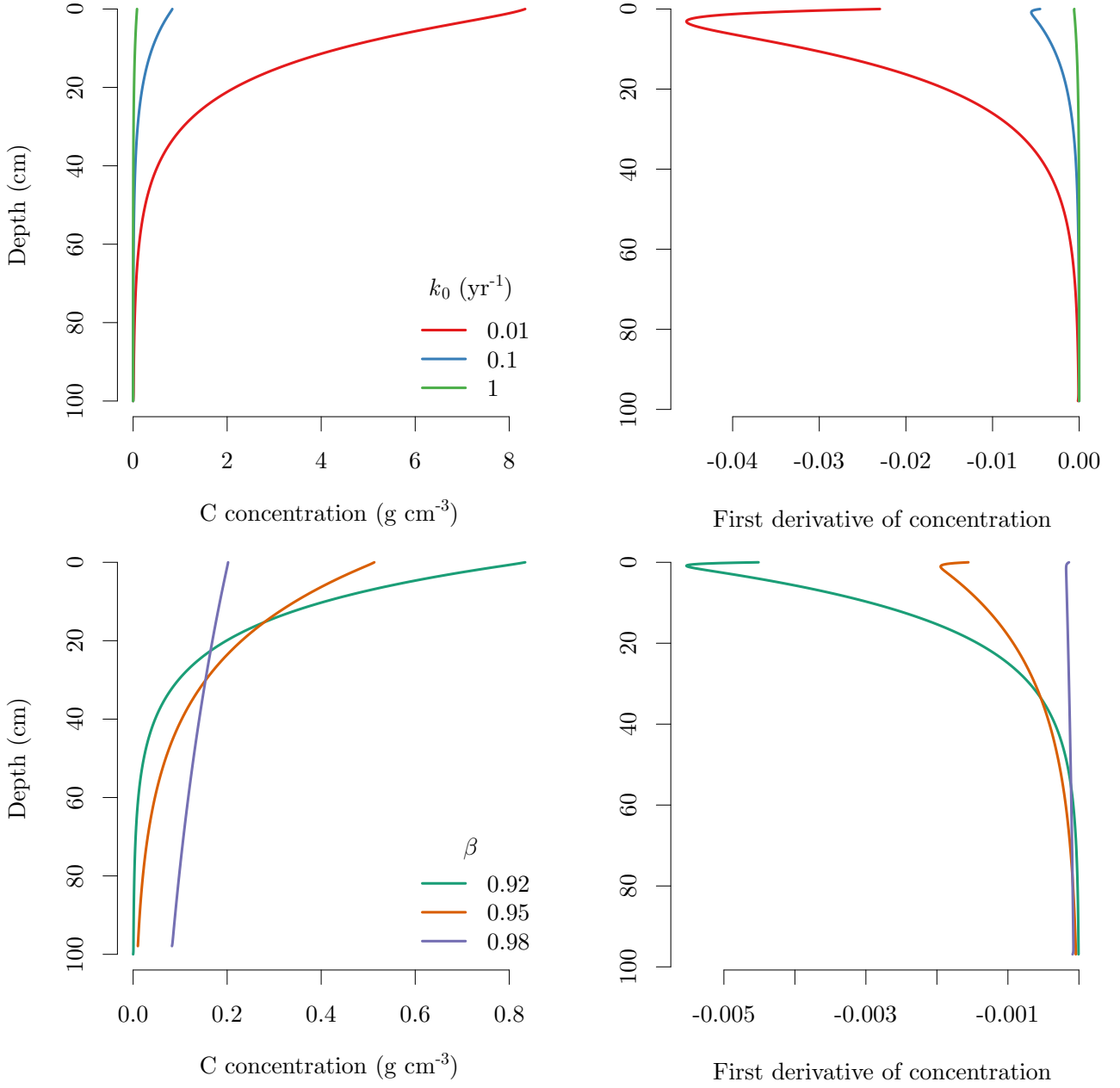


Figure 3: Numerical simulations of soil C depth profiles using the linear model with constant coefficients of equation 17. The top panels show C concentration and its first derivative with respect to depth for different functions representing decomposition rate $k(d)$ (equation 19). The different lines are the results of the model for different values of the maximum decomposition rate at the surface k_0 , with the value of $k_0 = 1 \text{ yr}^{-1}$ representing fast decomposition and $k_0 = 0.01 \text{ yr}^{-1}$ slow decomposition. The lower panels represent the results of simulation for different shapes of the root input profile according to equation 18, with the parameter $\beta = 0.98$ representing deep root inputs, and $\beta = 0.92$ shallow root inputs.

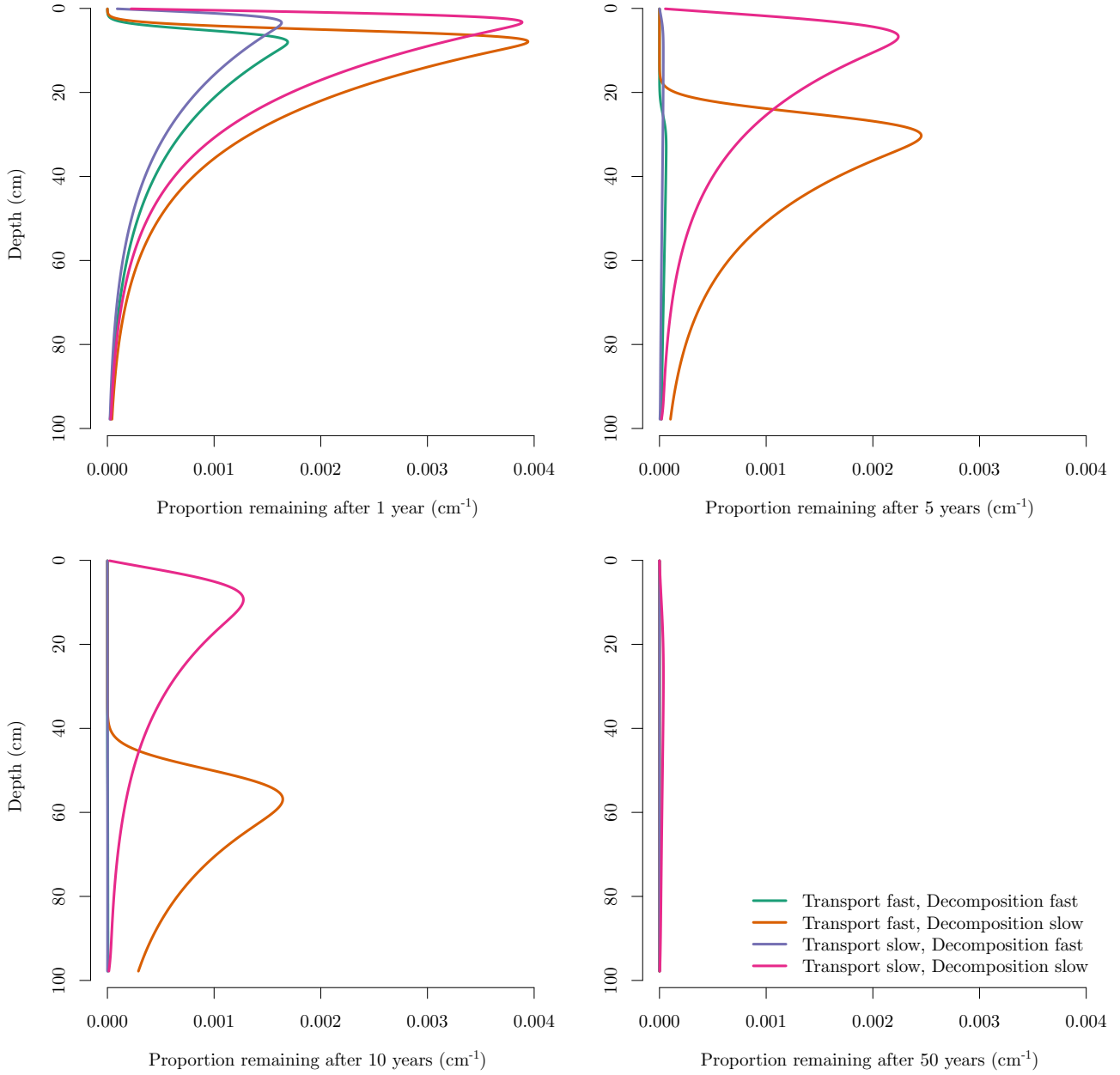


Figure 4: Proportion of C remaining in a soil profile of an amount of lateral inputs entering the soil at $t = 0$ represented with equation 18 with $\beta = 0.95$. After 50 years most of the carbon that entered at $t = 0$ is not present in the soil, even for the scenario with slow transport and decomposition rates.

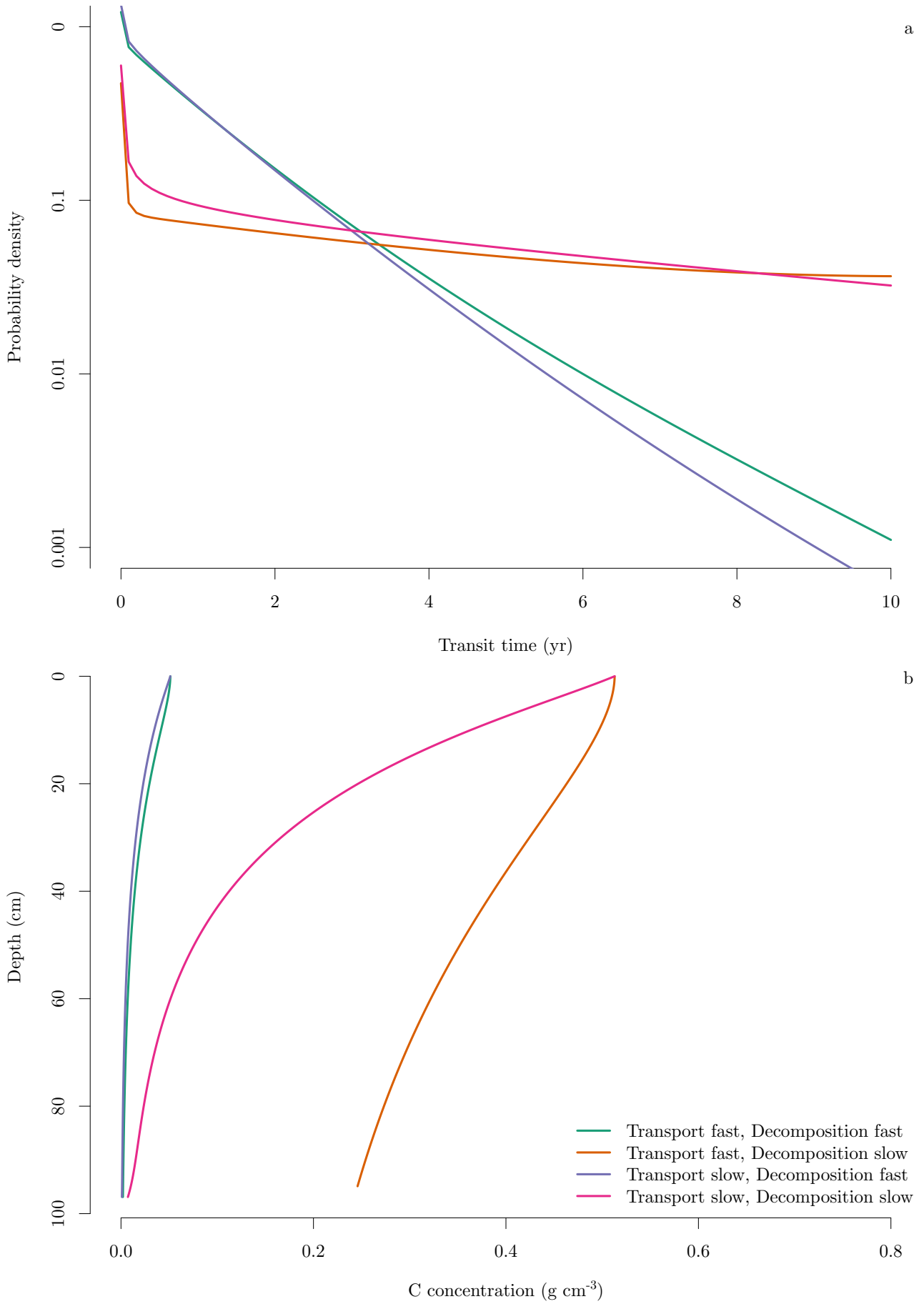


Figure 5: (a) Transit time distributions for four different scenarios of transport and decomposition in the subsoil. These distributions represent the proportion of C leaving the soil system at different times since the C entered the soil. Note the logarithmic y axis. (b) Values of C concentration along the depth profile at steady-state.

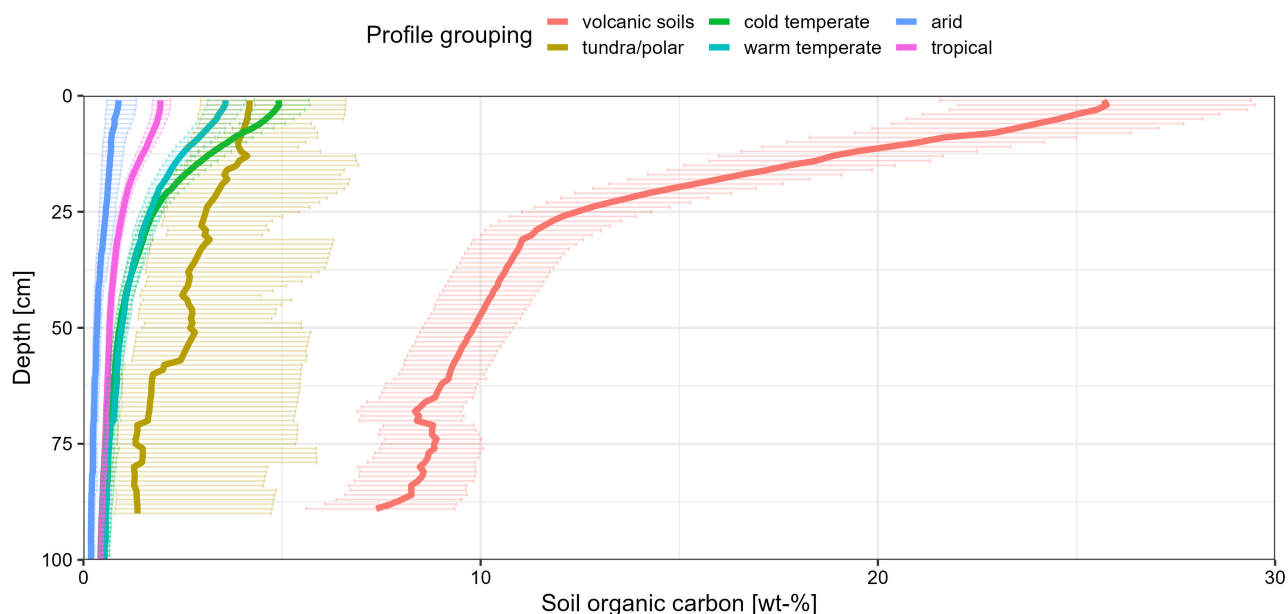


Figure 6: Soil carbon concentrations at different depths from the International Soil Radiocarbon Database, with data from 600 profiles aggregated by biogeographical regions. Thick lines for each group represent the mean across available observations and fitted to a spline curve. Horizontal lines represent standard deviation across available observations.

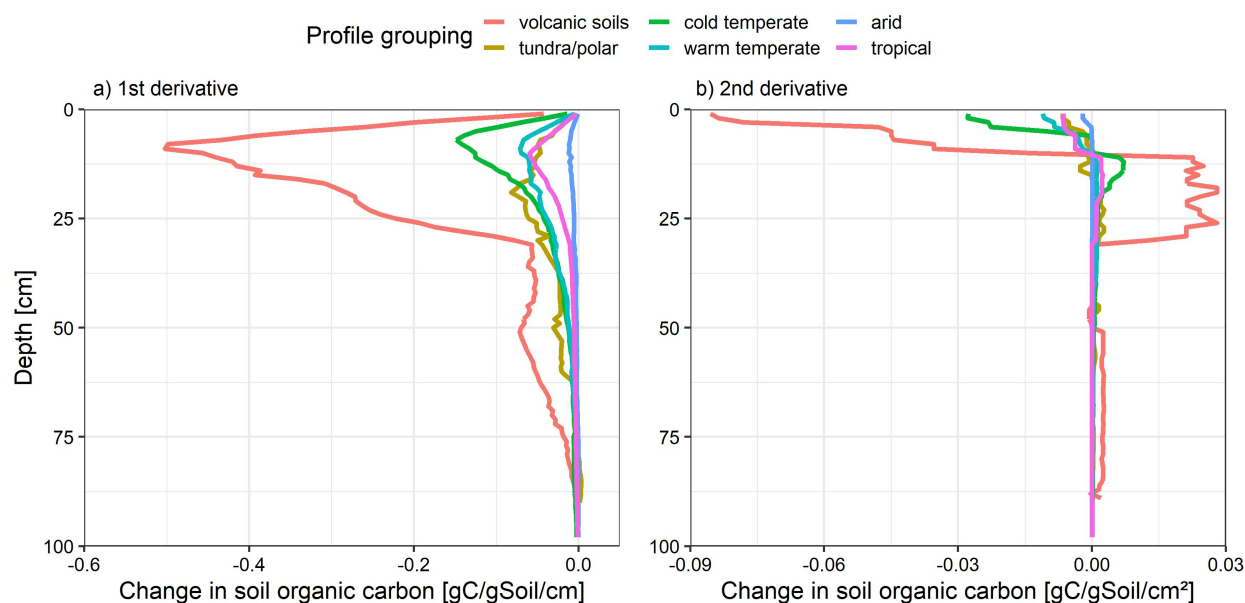


Figure 7: First and second derivative of soil C profiles extracted from ISRaD and grouped by biogeographical region, with the exception of volcanic soils.

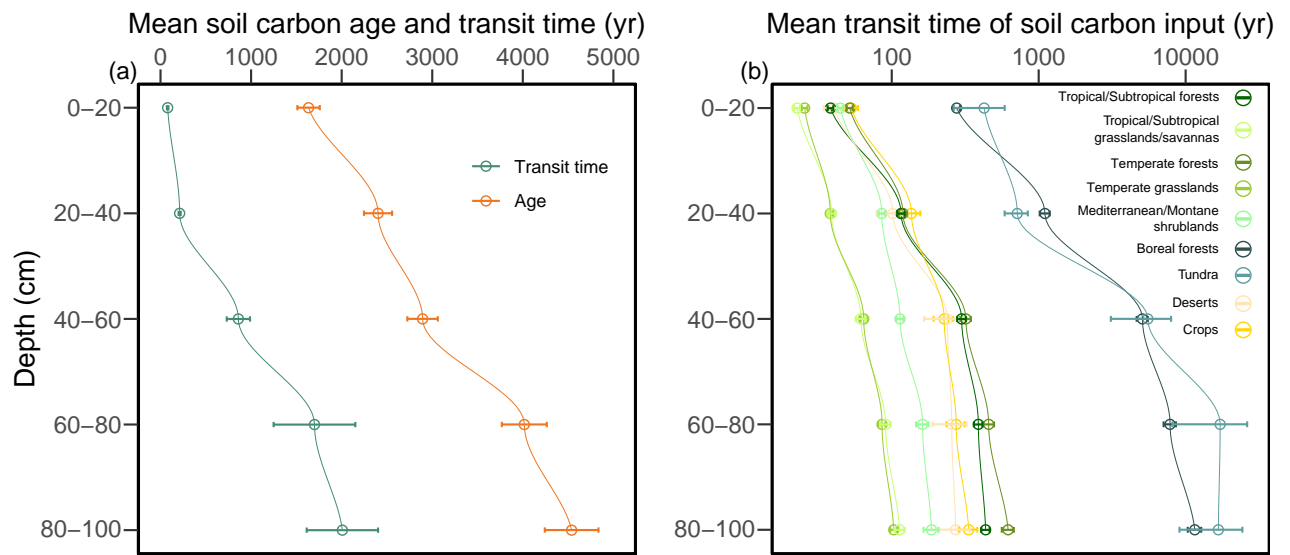


Figure 8: Estimates of mean age and mean transit time of carbon based on measurements of root inputs and soil radiocarbon obtained from ISRaD. The left panel shows global-scale average values of mean age and mean transit time. The right panel shows averages of mean transit time averaged by biome.